Flood risk reduction and flow buffering as ecosystem services:

I. Theory on a flow persistence indicator for watershed health

Meine van Noordwijk[1,2], Lisa Tanika[1], Betha Lusiana[1]

[1]{World Agroforestry Centre (ICRAF), SE Asia program, Bogor, Indonesia}

[2]{Wageningen University, Plant Production Systems, Wageningen, the Netherlands}

Correspondence to: Meine van Noordwijk (m.vannoordwijk@cgiar.org)

8   **Abstract 1**

9   Flood damage reflects insufficient adaptation of human presence and activity to

10   location and variability (inherent plus induced) of river flow. Increased variability and

11   reduced predictability of river flow is a common sign, in public discourse, of

12   degrading watersheds, combining increased flooding risk and reduced low flows. Flow

13   buffering in landscapes is commonly interpreted as ecosystem service, but needs

14   quantification. Geology, landscape form, soil porosity, litter layer and surface features,

15   drainage pathways, vegetation and space-time patterns of rainfall interact in complex

16   space-time patterns of riverflow, but the anthropogenic aspects tend to get discussed

17   on a one-dimensional scale of degradation and restoration. A strong tradition in public

18   discourse associates changes on such degradation-restoration axis with changes in tree

19   cover and/or forest quality, but the empirical evidence for such link that may exist at

20   high spatial resolution may not be a safe basis for securing required flow buffering in

21   landscapes at large. Capturing the relationship between the space-time patterns of

22   rainfall and riverflow in a single buffering indicator can help the way empirical

23   evidence is summarized and projected change in land use change scenarios is

24   evaluated. Where space-time details of rainfall remain unknown, a simpler approach is

25   needed. We present and discuss a candidate here for a single parameter representation

26   of the complex concept of watershed quality that does align short and long term

27   responses, and provides bounds to the levels of unpredicatibility. The dimensionless

28   FlowPer parameter (F_p) represents predictability of river flow. It is defined through a

29   recursive model of river flow, $Q_t = F_p Q_{t-1} + (1-F_p)(P_t - E_{tx})$, that relates the flow Q on

30   day t to that on the previous day (Q_{t-1}), and a term that reflects precipitation P on the

31   day itself and evapotranspiration E in a preceding time period, with Q, P and E

32   expressed in mm d^{-1}. When summed over one or more years, this recursive model

33   reflects the water balance ($\sum Q = \sum P - \sum E$), once changes in the storage term that can

34   dominate short term dynamics become negligible. F_p varies between 0 and 1, and can

35   be derived from a time-series of measured (or modeled) river flow data. In a

36   parsimonious interpretation that aligns with data sets that only exist of (daily) records

37   of riverflow, the spatially averaged precipitation term P_t and preceding cumulative

38   evapotranspiration since previous rain E_{tx} are treated as constrained but unknown,

39   stochastic variables. Without knowing when peak flows occur, the balance equation

40   suggests that a decrease in F_p from 0.9 to 0.8 means peak flow doubling from 10 to

41   20% of peak rainfall (minus its accompanying E_{tx}). Flood duration has a nonlinear

42   response to increases in F_p, as low F_p values lead to high peak flow of short duration,

43   and at high F_p values thresholds of flooding may never be reached. In a numerical

44   example a decrease in F_p led at most to an increase in expected flood duration by 3

45   days. As a potential indicator of watershed health (or quality), the F_p metric (or its

46   change over time from what appears to be the local norm) matches local knowledge

47   concepts, captures key aspects of the river flow dynamic and can be unambiguously

48   derived from empirical river flow data. Further exploration of responsiveness of F_p to

49   the interaction of land cover and the specific realization of space-time patterns of

50   rainfall in a limited observation period is needed to test the interpretation of Fp as

51   indicator of watershed health (or quality) in the way this is degrading or restoring

52   through land cover change and modifications of the overland and surface flow

53   pathways, given inherent properties such as geology, geomorphology and climate.

54   **1   Introduction**

55   Degradation of watersheds and its consequences for river flow regime and flooding intensity

56   and frequency are a widespread concern (Brauman et al., 2007; Bishop and Pagiola, 2012;

57   Winsemius et al., 2013). Current watershed rehabilitation programs that focus on increasing

58   tree cover in upper watersheds are only partly aligned with current scientific evidence of

59   effects of large-scale tree planting on streamflow (Ghimire et al., 2014; Malmer et al., 2010;

60   Palmer, 2009; van Noordwijk et al., 2007, 2015a; Verbist et al 2010). The relationship

61   between floods and change in forest quality and quantity, and the availability of evidence for

62   such a relationship at various scales has been widely discussed over the past decades

63   (Andréassian, 2004; Bruijnzeel, 2004; Bradshaw et al., 2007; van Dijk et al., 2009).

64   Measurements in Cote d'Ivoire, for example, showed strong scale dependence of runoff from

65   30-50% at 1 m^2 point scale, to 4% at 130 ha watershed scale, linked to spatial variability of

66   soil properties plus variations in rainfall patterns (Van de Giesen et al., 2000). The ratio

67   between peak and average flow decreases from headwater streams to main rivers in a

68   predictable manner; while mean annual discharge scales with (area)$^{1.0}$, maximum river flow

69   was found to scale with (area)$^{0.7}$ on average (Rodríguez-Iturbe and Rinaldo, 2001; van

70   Noordwijk et al., 1998). The determinants of peak flows are thus scale-dependent, with space-

71   time correlations in rainfall interacting with subcatchment-level flow buffering in peakflows

72   at any point along the river. Whether and where peakflows lead to flooding depends on the
73   capacity of the rivers to pass on peakflows towards downstream lakes or the sea, assisted by
74   riparian buffer areas with sufficient storage capacity (Baldasarre et al., 2013); reducing local
75   flooding risk by increased drainage increases flooding risk downstream, challenging the
76   nested-scales management of watersheds to find an optimal spatial distribution, rather then
77   minimization, of flooding probabilities. Well-studied effects of forest conversion on peak
78   flows in small upper stream catchments (Alila et al., 2009) do not necessarily translate to
79   flooding downstream. As summarized by Beck et al. (2013) meso- to macroscale catchment
80   studies (>1 and >10 000 km^2, respectively) in the tropics, subtropics, and warm temperate
81   regions have mostly failed to demonstrate a clear relationship between river flow and change
82   in forest area. Lack of evidence cannot be firmly interpreted as evidence for lack of effect,
83   however. A recent econometric study for Peninsular Malaysia by Tan-Soo et al. (2014)
84   concluded that, after appropriate corrections for space-time correlates in the data-set for 31
85   meso- and macroscale basins (554-28,643 km^2), conversion of inland rain forest to
86   monocultural plantations of oil palm or rubber increased the number of flooding days
87   reported, but not the number of flood events, while conversion of wetland forests to urban
88   areas reduced downstream flood duration. This Malaysian study may be the first credible
89   empirical evidence at this scale. The difference between results for flood duration and flood
90   frequency and the result for draining wetland forests warrant further scrutiny. Consistency of
91   these findings with river flow models based on a water balance and likely pathways of water
92   under the influence of change in land cover and land use has yet to be shown. Two recent
93   studies for Southern China confirm the conventional perspective that deforestation increases
94   high flows, but are contrasting in effects of reforestation. Zhou et al. (2010) analyzed a 50-
95   year data set for Guangdong Province in China and concluded that forest recovery had not
96   changed the annual water yield (or its underpinning water balance terms precipitation and
97   evapotransipiration), but had a statistically significant positive effect on dry season (low)
98   flows.   Liu et al. (2015), however, found for the Meijiang watershed (6983 km2) in
99   subtropical China that while historical deforestation had decreased the magnitudes of low
100 flows (daily flows $\leqq$ Q95%) by 30.1%, low flows were not significantly improved by
101 reforestation. They concluded that recovery of low flows by reforestation may take much
102 longer time than expected probably because of severe soil erosion and resultant loss of soil
103 infiltration capacity after deforestation. Changes in riverflow patterns over a limited period of
104 time can be the combined and interactive effects of variations in the local rainfall regime, land

105 cover effects on soil structure and engineering modifications of water flow, that can be teased

106 apart with modelling tools (Ma et al., 2014).

107 Lacombe et al. (2015) documented that the hydrological effects of natural regeneration differ

108 from those of plantation forestry, while forest statistics don't normally differentiate between

109 these different land covers. In a regression study of the high and low flow regimes in the

110 Volta and Mekong river basins Lacombe and McCartney (2016) found that in the variation

111 among tributaries various aspects of land cover and land cover change had explanatory power.

112 Between the two basins, however, these aspects differed. In the Mekong basin variation in

113 forest cover had no direct effect on flows, but extending paddy areas resulted in a decrease in

114 downstream low flows, probably by increasing evapotranspiration in the dry season. In the

115 Volta River Basin, the conversion of forests to crops (or a reduction of tree cover in the

116 existing parkland system) induced greater downstream flood flows. This observation is

117 aligned with the experimental identification of an optimal, intermediate tree cover from the

118 perspective of groundwater recharge in parklands in Burkina Faso (Ilstedt et al., 2016).

119 The statistical challenges of attribution of cause and effect in such data-sets are considerable

120 with land use/land cover interacting with spatially and temporally variable rainfall, geological

121 configuration and the fact that land use is not changing in random fashion or following any

122 pre-randomized design (Alila et al., 2009; Rudel et al., 2005). Hydrologicical analysis across

123 12 catchments in Puerto Rico by Beck et al. (2013) did not find significant relationships

124 between the change in forest cover or urban area, and change in various flow characteristics,

125 despite indications that regrowing forests increased evapotranspiration. Yet, the concept of a

126 'regulating function' on river flow regime for forests and other semi-natural ecosystems is

127 widespread. The considerable human and economic costs of flooding at locations and times

128 beyond where this is expected make the presumed 'regulating function' on flood reduction of

129 high value (Brauman et al., 2007) – if only we could be sure that the effect is real, beyond the

130 local scales (< 10 km^2) of paired catchments where ample direct empirical proof exists

131 (Bruijnzeel, 1990, 2004). These observations imply that percent tree cover (or other forest

132 related indicators) is probably not a good metric for judging the ecosystem services provided

133 by a watershed (of different levels of 'health'), and that a metric more directly reflecting

134 changes in river flow may be needed. Here we will explore a simple recursive model of river

135 flow (van Noordwijk et al., 2011) that (i) is focused on (loss of) predictability, (ii) can

136 account for the types of results obtained by the cited recent Malaysian study (Tan-Soo et al.,

137   2014), and (iii) may constitute a suitable performance indicator to monitor watershed 'health'

138   through time.

139   ⇨ Fig. 1

140   Figure 1 is compatible with a common dissection of risk as the product of hazard, exposure

141   and vulnerability. Extreme discharge events plus river-level engineering co-determine hazard,

142   while exposure depends on topographic position interacting with human presence, and

143   vulnerability can be modified by engineering at a finer scale and be further reduced by advice

144   to leave an area in high-risk periods. A recent study (Jongman et al., 2015) found that human

145   fatalities and material losses between 1980 and 2010 expressed as a share of the exposed

146   population and gross domestic product were decreasing with rising income. The planning

147   needed to avoid extensive damage requires quantification of the risk of higher than usual

148   discharges, especially at the upper tail end of the flow frequency distribution.

149   The statistical scarcity, per definition, of 'extreme events' and the challenge of data collection

150   where they do occur, make it hard to rely on empirical data as such. Existing data on flood

151   frequency and duration, as well as human and economic damage are influenced by

152   topography, human population density and economic activity, interacting with engineered

153   infrastructure (step 4 and 5 in Fig. 1), as well as the extreme rainfall events that are their

154   proximate cause. Subsidence due to groundwater extraction in urban areas of high population

155   density is a specific problem for a number of cities built on floodplains (such as Jakarta and

156   Bangkok), but subsidence of drained peat areas has also been found to increase flooding risks

157   elsewhere (Sumarga et al., 2016). Common hydrological analysis of flood frequency (called 1

158   in 10-, 1 in 100-, 1 in 1000-year flood events, for example) doess not separately attribute

159   flood magnitude to rainfall and land use properties, and analysis of likely change in flood

160   frequencies in the context of climate change adaptation has been challenging (Milly et al.,

161   2002; Ma et al., 2014). There is a lack of simple performance indicators for watershed health

162   at its point of relating precipitation P and river flow Q (step 2 in Fig. 1) that align with local

163   observations of river behavior and concerns about its change and that can reconcile local,

164   public/policy and scientific knowledge, thereby helping negotiated change in watershed

165   management (Leimona et al., 2015). The behavior of rivers depends on many climatic (step 1

166   in Figure 1) and terrain factors (step 7-9 in Figure 1) that make it a challenge to differentiate

167   between anthropogenically induced ecosystem structural change and soil degradation (step

168   7a) on one hand and intrinsic variability on the other. Arrow 10 in Figure 1 represents the

169   direct influence of climate on vegetation, but also a possible reverse influence (van Noordwijk

et al., 2015b). Hydrological models tend to focus on predicting hydrographs at one or more temporal scales, and are usually tested on data-sets from limited locations. Despite many decades (if not centuries) of hydrological modeling, current hydrologic theory, models and empirical methods have been found to be largely inadequate for sound predictions in ungauged basins (Hrachowitz et al., 2013). Efforts to resolve this through harmonization of modelling strategies have so far failed. Existing models differ in the number of explanatory variables and parameters they use, but are generally dependent on empirical data of rainfall that are available for specific measurement points but not at the spatial resolution that is required for a close match between measured and modeled river flow. Spatially explicit models have conceptual appeal (Ma et al., 2010) but have too many degrees of freedom and too many opportunities for getting right answers for wrong reasons if used for empirical calibration (Beven, 2011). Parsimonious, parameter-sparse models are appropriate for the level of evidence available to constrain them, but these parameters are themselves implicitly influenced by many aspects of existing and changing features of the watershed, making it hard to use such models for scenario studies of interacting land use and climate change. Here we present a more direct approach deriving a metric of flow predictability that can bridge local concerns and concepts to quantified hydrologic function: the 'flow persistence' parameter (step 2 in Figure 1).

In this contribution to the debate we will first define the metric 'flow persistence' in the context of temporal autocorrelation of river flow and then derive a way to estimate its numerical value. In part II we will apply the algorithm to river flow data for a number of contrasting meso-scale watersheds. In the discussion of this paper we will consider the new flow persistence metric in terms of three groups of criteria for usable knowledge (Clark et al., 2011; Lusiana et al., 2011; Leimona et al., 2015) based on salience (1,2), credibility (3,4) and legitimacy (5-7):

1. Does flow persistence relate to important aspects of watershed behavior?

2. Does it's quantification help to select management actions?

3. Is there consistency of numerical results?

4. How sensitive is it to bias and random error in data sources?

5. Does it match local knowledge?

6. Can it be used to empower local stakeholders of watershed management?

201   7. Can it inform local risk management?

202 Questions 3 and 4 will get specific attention in part II.

2 Recursive river flow model and flow persistence

2.1 Basic equations

205 One of the easiest-to-observe aspects of a river is its day-to-day fluctuation in waterlevel,
206 related to the volumetric flow (discharge) via rating curves (Maidment, 1992). Without
207 knowing details of upstream rainfall and the pathways the rain takes to reach the river,
208 observation of the daily fluctuations in waterlevel allows important inferences to be made. It
209 is also of direct utility: sudden rises can lead to floods without sufficient warning, while rapid
210 decline makes water utilization difficult. Indeed, a common local description of watershed
211 degradation is that rivers become more 'flashy' and less predictable, having lost a buffer or
212 'sponge' effect (Joshi et al., 2004; Ranieri et al., 2004; Rahayu et al., 2013). The probably
213 simplest model of river flow at time t, Q_t, is that it is similar to that of the day before (Q_{t-1}), to
214 the degree F_p, a dimensionless parameter called 'flow persistence' (van Noordwijk et al.,
215 2011) plus an additional stochastic term $Q_{a,t}$:

216 $$Q_t = F_p Q_{t-1} + Q_{a,t} \qquad [1].$$

217 Q_t is for this analysis expressed in mm d^{-1}, which means that measurements in m^3 s^{-1} need to
218 be divided by the relevant catchment area, with appropriate unit conversion. If river flow were
219 constant, it would be perfectly predictable, i.e. F_p would be 1.0 and $Q_{a,t}$ zero; in contrast, an
220 F_p-value equal to zero and $Q_{a,t}$ directly reflecting erratic rainfall represents the lowest possible
221 level of predictability.

222 The F_p parameter is conceptually identical to the 'recession constant' commonly used in
223 hydrological models, typically assessed during an extended dry period when the $Q_{a,t}$ term is
224 negligible and streamflow consists of baseflow only (Tallaksen, 1995); empirical deviations
225 from a straight line in a plot of the logarithm of Q against time are common and point to
226 multiple rather than a single groundwater pool that contributes to base flow. With increasing
227 size of a catchment area it is increasingly likely that there indeed are multiple, partly
228 independent groundwater contributions.

229   As we will demonstrate in a next section, it is possible to derive F_p even when $Q_{a,t}$ is not

230   negligible. In climates without distinct dry season this is essential; elsewhere it allows a

231   comparison of apparent F_p between wet and dry parts of the hydrologic year. A possible

232   interpretation, to be further explored, is that decrease over the years of F_p indicates 'watershed

233   degradation' (i.e. greater contrast between high and low flows), and an increase

234   'improvement' or 'rehabilitation' (i.e. more stable flows).

235   If we consider the sum of river flow over a period of time (from 1 to T) we obtain

236    $\Sigma_1^T Q_t = F_p \Sigma_1^T Q_{t-1} + \Sigma_1^T Q_{a,t}$ [2].

237   If the period is sufficiently long period for Q_T minus Q_0 to be negligibly small relative to the

238   sum over all t's, we may equate $\Sigma_1^T Q_t$ with $\Sigma_1^T Q_{t-1}$ and obtain a first way of estimating the F_p

239   value:

240    $F_p = 1 - \Sigma_1^T Q_{a,t} / \Sigma_1^T Q_t$ [3].

241   Rearranging Eq.(3) we obtain

242    $\Sigma_1^T Q_{a,t} = (1 - F_p) \Sigma_1^T Q_t$ [4].

243   The F_p term is equivalent with one of several ways to separate baseflow from peakflows. The

244    $\Sigma Q_{a,t}$ term reflects the sum of peak flows in mm, while $F_p \Sigma Q_t$ reflects the sum of base flow,

245   also in mm. For $F_p = 1$ (the theoretical maximum) we conclude that all $Q_{a,t}$ must be zero, and

246   all flow is 'base flow'.

247   The stochastic $Q_{a,t}$ can be interpreted in terms of what hydrologists call 'effective rainfall'

248   (i.e. rainfall minus on-site evapotranspiration, assessed over a preceding time period tx since

249   previous rain event):

250    $Q_t = F_p Q_{t-1} + (1-F_p)(P_{tx} - E_{tx})$ [5].

251   Where P_{tx} is the (spatially weighted) precipitation (assuming no snow or ice, which would

252   shift the focus to snowmelt) in mm d^{-1}; E_{tx} , also in mm d^{-1}, is the preceding

253   evapotranspiration that allowed for infiltration during this rainfall event (*i.e.*

254   evapotranspiration since the previous soil-replenishing rainfall that induced empty pore space

255   in the soil for infiltration and retention), or replenishment of a waterfilm on aboveground

256   biomass that will subsequently evaporate. More complex attributions are possible, aligning

257   with the groundwater replenishing bypassflow and the water isotopic fractionation involved

258   in evaporation (Evaristo et al., 2015).

259 The consistency of multiplying effective rainfall with $(1-F_p)$ can be checked by considering

260 the geometric series $(1-F_p)$, $(1-F_p) F_p$, $(1-F_p) F_p^2$, …, $(1-F_p) F_p^n$ which adds up to $(1-F_p)(1 -$

261 $F_p^n)/(1-F_p)$ or $1 - F_p^n$. This approaches 1 for large n, suggesting that all of the water attributed

262 to time t, *i.e.* $P_t – E_{tx}$, will eventually emerge as river flow. For $F_p = 0$ all of $(P_t – E_{tx})$ emerges

263 on the first day, and riverflow is as unpredictable as precipitation itself. For $F_p = 1$ all of $(P_t –$

264 $E_{tx})$ contributes to the stable daily flow rate, and it takes an infinitely long period of time for

265 the last drop of water to get to the river. For declining F_p, $(1 > F_p > 0)$, river flow gradually

266 becomes less predictable, because a greater part of the stochastic precipitation term

267 contributes to variable rather than evened-out river flow.

268 Taking long term summations of the right- and left- hand sides of Eq.(5) we obtain:

269 $\Sigma Q_t = \Sigma(F_p Q_{t-1} + (1-F_p)(P_t – E_{tx})) = F_p \Sigma Q_{t-1} + (1-F_p)(\Sigma P_t – \Sigma E_{tx}))$ [6].

270 Which is consistent with the basic water budget, $\Sigma Q = \Sigma P – \Sigma E$, at time scales long enough

271 for changes in soil water buffer stocks to be ignored. As such the total annual, and hence the

272 mean daily river flow are independent of F_p. This does not preclude that processes of

273 watershed degradation or restoration that affect the partitioning of P over Q and E also affect

274 F_p.

275 **2.2 Low flows**

276 The lowest flow expected in an annual cycle is $Q_x F_p^{Nmax}$ where Q_x is flow on the first day

277 without rain and N_{max} the longest series of dry days. Taken at face value, a decrease in F_p has

278 a strong effect on low-flows, with a flow of 10% of Q_x reached after 45, 22, 14, 10, 8 and 6

279 days for $F_p = 0.95, 0.9, 0.85, 0.8, 0.75$ and 0.7, respectively. However, the groundwater

280 reservoir that is drained, equalling the cumulative dry season flow if the dry period is

281 sufficiently long, is $Q_x/(1-F_p)$. If F_p decreases to F_{px} but the groundwater reservoir (Res $=$

282 $Q_x/(1-F_p)$) is not affected, initial flows in the dry period will be higher $(Q_x F_{px}^i (1-F_{px})$ Res $>$

283 $Q_x F_p^i (1-F_p)$ Res for $i < \log((1-F_{px})/(1-F_p))/\log(F_p/F_{px}))$. It thus matters how low flows are

284 evaluated: from the perspective of the lowest level reached, or as cumulative flow. The

285 combination of climate, geology and land form are the primary determinants of cumulative

286 low flows, but if land cover reduces the recharge of groundwater there may be impacts on dry

287 season flow, that are not directly reflected in F_p.

288 If a single F_p value would account for both dry and wet season, the effects of changing F_p on

289 low flows may well be more pronounced than those on flood risk. Empirical tests are needed

290 of the dependence of F_p on Q (see below). Analysis of the way an aggregate F_p depends on

291 the dominant flow pathways provides a basis for differentiating F_p within a hydrologic year.

293 2.3 Flow-pathway dependence of flow persistence

294 The patch-level partitioning of water between infiltration and overlandflow is further

295 modified at hillslope level, with a common distinciton between three pathways that reach

296 streams: overland flow, interflow and groundwater flow (Band et al., 1993; Weiler and

297 McDonnell, 2004). An additional interpretation of Eq.(1), potentially adding to our

298 understanding of results but not needed for analysis of empirical data, can be that three

299 pathways of water through a landscape contribute to river flow (Barnes, 1939): groundwater

300 release with $F_{p,g}$ values close to 1.0, overland flow with $F_{p,o}$ values close to 0, and interflow

301 with intermediate $F_{p,i}$ values.

302 $Q_t = F_{p,g} Q_{t-1,g} + F_{p,i} Q_{t-1,i} + F_{p,o} Q_{t-1,o} + Q_{a,t}$ [7],

303 $F_p = (F_{p,g} Q_{t-1,g} + F_{p,i} Q_{t-1,i} + F_{p,o} Q_{t-1,o})/Q_{t-1}$ [8].

304 On this basis a decline or increase in overall weighted average F_p can be interpreted as

305 indicator of a shift of dominant runoff pathways through time within the watershed. Dry

306 season flows are dominated by $F_{p,g}$. The effective F_p in the rainy season can be intyerpreted as

307 indicating the relative importance of the other two flow pathways. F_p reflects the fractions of

308 total river flow that are based on groundwater, overland flow and interflow pathways:

309 $F_p = F_{p,g} (\Sigma Q_{t,g} / \Sigma Q_t) + F_{p,o} (\Sigma Q_{t,o} / \Sigma Q_t) + F_{p,i} (\Sigma Q_{t,i} / \Sigma Q_t)$ [9].

310 Beyond the type of degradation of the watershed that, mostly through soil compaction, leads

311 to enhanced infiltration-excess (or Hortonian) overland flow (Delfs et al., 2009), saturated

312 conditions throughout the soil profile may also induce overland flow, especially near valley

313 bottoms (Bonell, 1993; Bruijnzeel, 2004). Thus, the value of $F_{p,o}$ can be substantially above

314 zero if the rainfall has a significant temporal autocorrelation, with heavy rainfall on

315 subsequent days being more likely than would be expected from general rainfall frequencies.

316 If rainfall following a wet day is more likely to occur than following a dry day, as is

317 commonly observed in Markov chain analysis of rainfall patterns (Jones and Thornton, 1997;

318 Bardossy and Plate, 1991), the overland flow component of total flow will also have a partial

319 temporal autocorrelation, adding to the overall predictability of river flow. In a hypothetical

320 climate with evenly distributed rainfall, we can expect F_p to be 1.0 even if there is no

321   infiltration and the only pathway available is overland flow. Even with rainfall that is variable

322   at any point of observation but has low spatial correlation it is possible to obtain F_p values of

323   (close to) 1.0 in a situation with (mostly) overland flow (Ranieri at al., 2004).

324   **3. Methods**

325   **3.1 Numerical example**

326   Figure 2 provides an example of the way a change in F_p values (based on Eq. 1) influences the

327   visual pattern of river flow for a unimodal rainfall regime with a well-developed dry season.

328   The increasing 'spikedness' of the graph as F_p is lowered indicates reduced predictability of

329   flow on any given day during the wet season on the basis of the flow on the preceding day. A

330   bi-plot of river flow on subsequent days for the same simulations (Fig. 3) shows two main

331   effects of reducing the F_p value: the scatter increases, and the slope of the lower envelope

332   containing the swarm of points is lowered (as it equals F_p). Both of these changes can provide

333   entry points for an algorithm to estimate F_p from empirical time series, provided the basic

334   assumptions of the simple model apply and the data are of acceptable quality (see Section 3

335   below). For the numerical example shown in Fig. 2, the maximum daily flow doubled from 50

336   to 100 mm when the F_p value decreased from a value close to 1 (0.98) to nearly 0.

337   ⇨ Fig. 2
338   ⇨ Fig. 3

339   **3.2 Flow persistence as a simple flood risk indicator**

340   For numerical examples (implemented in a spreadsheet model) flow on each day can be

341   derived as:

342   $Q_t = \Sigma_j^t \; F_p^{t-j} \; (1-F_p) \; p_j \, P_j$ [10].

343   Where p_j reflects the occurrence of rain on day j (reflecting a truncated sine distribution for

344   seasonal trends) and P_j is the rain depth (drawn from a uniform distribution). From this model

345   the effects of F_p (and hence of changes in F_p) on maximum daily flow rates, plus maximum

346   flow totals assessed over a 2-5 d period, was obtained in a Monte Carlo process (without

347   Markov autocorrelation of rainfall in the default case – see below). Relative flood protection

348   was calculated as the difference between peak flows (assessed for 1-5 d duration after a 1 year

349   'warm-up' period) for a given F_p versus those for $F_p = 0$, relative to those at $F_p = 0$.

350   **3.3 An algorithm for deriving F_p from a time series of stream flow data**

351 Equation (3) provides a first method to derive F_p from empirical data if these cover a full

352 hydrologic year. In situations where there is no complete hydrograph and/or in situations

353 where we want to quantify F_p for shorter time periods (e.g. to characterise intraseasonal flow

354 patterns) and the change in the storage term of the water budget equation cannot be ignored,

355 we need an algorithm for estimating F_p from a series of daily Q_t observations.

356 Where rainfall has clear seasonality, it is attractive and indeed common practice to derive a

357 groundwater recession rate from a semi-logarithmic plot of Q against time (Tallaksen, 1995).

358 As we can assume for such periods that $Q_{a,t} = 0$, we obtain $F_p = Q_t / Q_{t-1}$, under these

359 circumstances. We cannot be sure, however, that this $F_{p,g}$ estimate also applies in the rainy

360 season, because overall wet-season F_p will include contributions by $F_{p,o}$ and $F_{p,i}$ as well

361 (compare Eq. 9). In locations without a distinct dry season, we need an alternative method.

362 A biplot of Q_t against Q_{t-1} (as in Fig. 3) will lead to a scatter of points above a line with slope

363 F_p, with points above the line reflecting the contributions of $Q_{a,t} > 0$, while the points that plot

364 on the F_p line itself represent $Q_{a,t} = 0$ mm d^{-1}. There is no independent source of information

365 on the frequency at which $Q_{a,t} = 0$, nor what the statistical distribution of $Q_{a,t}$ values is if it is

366 non-zero. Calculating back from the Q_t series we can obtain an estimate ($Q_{a,Fptry}$) of $Q_{a,t}$ for

367 any given estimate ($F_{p,try}$) of F_p, and select the most plausible F_p value. For high $F_{p,try}$

368 estimates there will be many negative $Q_{a,Fptry}$ values, for low $F_{p,try}$ estimates all $Q_{a,Fptry}$ values

369 will be larger. An algorithm to derive a plausible F_p estimate can thus make use of the

370 corresponding distribution of 'apparent Q_a' values as estimates of $F_{p,try}$, calculated as $Q_{a,try} =$

371 $Q_t - F_{p,try} Q_{t-1}$. While $Q_{a,t}$ cannot be negative in theory, small negative Q_a estimates are likely

372 when using real-world data with their inherent errors. The FlowPer F_p algorithm (van

373 Noordwijk et al., 2011) derives the distribution of $Q_{add,Fptry}$ estimates for a range of $F_{p,try}$

374 values (Fig. 4B) and selects the value $F_{p,try}$ that minimizes the variance $Var(Q_{a,Fptry})$ (or its

375 standard deviation) (Fig. 4C). It is implemented in a spreadsheet workbook that can be

376 downloaded from the ICRAF website (http://www.worldagroforestry.org/output/flowper-

377 flow-persistence-model)

378 ➔Fig. 4

379 A consistency test is needed that the high-end Q_t values relate to Q_{t+1} in the same was as do

380 low or medium Q_t values. Visual inspection of Q_{t+1} versus Q_t, with the derived F_p value,

381 provides a qualitative view of the validity of this assumption. The F_p algorithm can be applied

382 to any population of (Q_{t-1}, Q_t) pairs, e.g. selected from a multiyear data set on the basis of 3-

383 month periods within the hydrological year.

4 Results

4.1 Flood intensity and duration

386 Figure 5 shows the effect of F_p values in the range 0 to 1 on the maximum flows obtained

387 with a random time series of 'effective rainfall', compared to results for $F_p = 0$. Maximum

388 flows were considered at time scales of 1 to 5 days, in a moving average routine. This way a

389 relative flood protection, expressed as reduction of peak flow, could be related to F_p (Fig.

390 5A).

391   ⇨ Fig. 5

392 Relative flood protection rapidly decreased from its theoretical value of 100% at $F_p = 1$ (when

393 there was no variation in river flow), to less than 10% at F_p values of around 0.5. Relative

394 flood protection was slightly lower when the assessment period was increased from 1 to 5

395 days (between 1 and 3 d it decreased by 6.2%, from 3 to 5 d by a further 1.3%). Two

396 counteracting effects are at play here: a lower F_p means that a larger fraction $(1-F_p)$ of the

397 effective rainfall contributes to river flow, but the increased flow is less persistent. In the

398 example the flood protection in situations where the rainfall during 1 or 2 d causes the peak is

399 slightly stronger than where the cumulative rainfall over 3-5 d causes floods, as typically

400 occurs downstream.

401 As we expect from equation 5 that peak flow is to $(1-F_p)$ times peak rainfall amounts, the

402 effect of a change in F_p not only depends on the change in F_p that we are considering, but also

403 on its initial value. Higher initial F_p values will lead to more rapid increases in high flows for

404 the same reduction in F_p (Fig. 5B). However, flood duration rather responds to changes in F_p

405 in a curvilinear manner, as flow persistence implies flood persistence (once flooding occurs),

406 but the greater the flow persistence the less likely such a flooding threshold is passed (Fig.

407 5C). The combined effect may be restricted to about 3 d of increase in flood duration for the

408 parameter values used in the default example, but for different parametrization of the

409 stochastic ε other results might be obtained.

4.2 Algorithm for Fp estimates from river flow time series

The algorithm has so far returned non-ambiguous F_p estimates on any modelled time series data of river flow, as well as for all empirical data set we tested (including all examples tested in part II), although there proably are data sets on which it can breakdown. Visual inspection of Q_{t-1}/Q_t biplots (as in Fig. 3) can provide clues to non-homogenous data sets, and to potential situations where effective F_p depends on flow level Q_t.and where data are not consisten with a straigh-line lower envelope. Where river flow estimates were derived from a model with random elements, however, variation in F_p estimates was observed, that sugegsts that specific aspects of actual rainfall, beyond the basic characteristics of a watershed and its vegetation, do have at least some effect. Such effects deserve to be further explored for a set of case studies, as their strength probably depends on context.

5 Discussion

We will discuss the flow persistence metric based on the questions raised from the perspectives of salience, credibility and legitimacy.

5.1 Salience

Key *salience* aspects are "Does flow persistence relate to important aspects of watershed behavior?" and "Does it help to select management actions?". A major finding in the derivation of F_p was that the flow persistence measured at daily time scale can be logically linked to the long-term water balance, and that the proportion of peak rainfall that translates to peak river flow equals the complement of flow persistence. This feature links effects on floods of changes in watershed quality to effects on low flows, although not in a linear relationship. The F_p parameter as such does not predict when and where flooding will occur, but it does help to assess to what extent another condition of the watershed, with either higher or lower F_p would translate the same rainfall into larger or small peak waterflows. This is salient, especially if the relative contributions of (anthropogenic) land cover and the (exogenous, probabilistic) specifics of the rainfall pattern can be further teased apart (see part II). Where F_p may describe the descending branch of hydrographs at a relevant time scale, details of the ascending branch beyond the maximum daily flow reached may be relevant for reducing flood damage, and may require more detailed study at higher tempoeral resolution.

439   A key strength of our flow persistence parameter, that it can be derived from observing river
440   flow at a single point along the river, without knowledge of rainfall events and catchment
441   conditions, is also its major weakness. If rainfall data exist, and especially rainfall data that
442   apply to each subcatchment, the Q_a term doesn't have to be treated as a random variable and
443   event-specific information on the flow pathways may be inferred for a more precise account
444   of the hydrograph. But for the vast majority of rivers in the tropics, advances in remotely
445   sensed rainfall data are needed to achieve that situation and F_p may be all that is available to
446   inform public debates on the relation between forests and floods.

447   Figures 2 and 6 show that most of the effects of a decreasing F_p value on peak discharge
448   (which is the basis for downstream flooding) occur between F_p values of 1 and 0.7, with the
449   relative flood protection value reduced to 10% when F_p reaches 0.5. As indicated in Fig. 1,
450   peak discharge is only one of the factors contributing to flood risk in terms of human
451   casualties and physical damage. The F_p value has an inverse effect on the fraction of recent
452   rainfall that becomes river flow, but the effect on peak flows is less, as higher F_p values imply
453   higher base flow. The way these counteracting effects balance out depends on details of the
454   local rainfall pattern (including its Markov chain temporal autocorrelation), as well as the
455   downstream topography and risk of people being at the wrong time at a given place, but the F_p
456   value is en efficient way of summarizing complex land use mosaics and upstream topography
457   in its effect on river flow. The difference between wet-season and dry-season F_p deserves
458   further analysis. In climates with a real rainless dry-season, dry season F_p is dominated by the
459   groundwater release fraction of the watershed, regardless of land cover, while in wet season it
460   depends on the mix (weighted average) of flow pathways. The degree to which F_p can be
461   influenced by land cover needs to be assessed for each landscape and land cover combination,
462   including the locally relevant forest and forest derived land classes, with their effects on
463   interception, soil infiltration and time pattern of transpiration. The F_p value can summarize
464   results of models that explore land use change scenarios in local context. To select the
465   specific management actions that will maintain or increase F_p a locally calibrated land
466   use/hydrology model is needed, such as GenRiver or SWAT (Yen et al., 2015).

467   Although a higher F_p value will in most cases be desirable (and a decrease in F_p undesirable),
468   we may expect that downstream biota have adjusted to the pre-human flow conditions and its
469   inherent F_p and variability. Decreased variability of flow achieved by engineering
470   interventions (e.g. a reservoir with constant release of water to generate hydropower) may

471   have negative consequences for fish and other biota (Richter et al., 2003; McCluney et al,
472   2014).

5.2 Credibility

474   Key *credibility* questions are "Consistency of numerical results?" and "How sensitive are
475   results to bias and random error in data sources?". This is further discussed in part II, after a
476   number of case studies has been studied. The main conclusions are that intra-annual
477   variability of F_p values between wet and dry seasons was around 0.2 in the case studies,
478   interannual variability in either annual or seasonal F_p was generally in the 0.1 range, while the
479   difference between observed and simulated flow data as basis for F_p calculations was mostly
480   less than 0.1. With current methods, it seems that effects of land cover change on flow
481   persistence that shift the F_p value by about 0.1 are the limit of what can be asserted from
482   empirical data (with shifts of that order in a single year a warning sign rather than a firmly
483   established change). When derived from observed river flow data F_p is suitable for monitoring
484   change (degradation, restoration) and can be a serious candidate for monitoring performance
485   in outcome-based ecosystem service management contracts. In interpreting changes in F_p as
486   caused by changes in the condition in the watershed, however, changes in specific properties
487   of the rainfall regime must be excluded. At the scale of paired catchment studies this
488   assumption may be reasonable, but in temporal change (or using specific events as starting
489   point for analysis), it is not easy to disentangle interacting effects (Ma et al., 2014). Recent
490   evidence that vegetation not only responds to, but also influences rainfall (arrow 10 in Figure
491   1; van Noordwijk et al., 2015b) further complicates the analysis across scales.

5.3 Legitimacy

493   *Legitimacy* aspects are "Does it match local knowledge?" and "Can it be used to empower
494   local stakeholders of watershed management?" and "Can it inform risk management?". As the
495   F_p parameter captures the predictability of river flow that is a key aspect of degradation
496   according to local knowledge systems, its results are much easier to convey than full
497   hydrographs or excedance probabilities of flood levels. By focusing on observable effects at
498   river level, rather than prescriptive recipes for land cover ("reforestation"), the F_p parameter
499   can be used to more effectively compare the combined effects of land cover change, changes
500   in the riparian wetlands and engineered water storage reservoirs, in their effect on flow
501   buffering. It is a candidate for shifting environmental service reward contracts from input to

502 outcome based monitoring (van Noordwijk et al., 2012). As such it can be used as part of a

503 negotiation support approach to natural resources management in which leveling off on

504 knowledge and joint fact finding in blame attribution are key steps to negotiated solutions that

505 are legitimate and seen to be so (van Noordwijk et al., 2013; Leimona et al., 2015).

506 Quantification of F_p can help assess tactical management options (Burt et al., 2014) as in a

507 recent suggestion to minimize negative downstream impacts of forestry operations on stream

508 flow by avoiding land clearing and planting operations in locally wet La Niña years. But the

509 most challenging aspect of the management of flood, as any other environmental risk, is that

510 the frequency of disasters is too low to intuitively influence human behavior where short-term

511 risk taking benefits are attractive. Wider social pressure is needed for investment in watershed

512 health (as a type of insurance premium) to be mainstreamed, as individuals waiting to see

513 evidence of necessity are too late to respond. In terms of flooding risk, actions to restore or

514 retain watershed health can be similarly justified as insurance premium. It remains to be seen

515 whether or not the transparency of the F_p metric and its intuitive appeal are sufficient to make

516 the case in public debate when opportunity costs of foregoing reductions in flow buffering by

517 profitable land use are to be compensated and shared (Burt et al., 2014).

518 **5.4 Conclusions and specific questioons for a set of case studies**

519 In conclusion, the F_p metric appears to allow an efficient way of summarizing complex

520 landscape processes into a single parameter that reflects the effects of landscape management.

521 Flow persistence is the result of rainfall persistence and the temporal delay provided by the

522 pathway water takes through the soil and the river system. High flow persistence indicates a

523 reliable water supply, while minimizing peak flow events. Wider tests of the F_p metric as

524 boundary object in science-practice-policy boundary chains (Kirchoff et al 2015; Leimona et

525 al., 2015) are needed. Further tests for specific case studies can clarify how changes in tree

526 cover (deforestation, reforestation, agroforestation) in different contexts influence river flow

527 dynamics and F_p values. Sensitivity to specific realizations of underlying time-space rainfall

528 patterns needs to be quantified, before changes in F_p can be attributed to 'watershed quality',

529 rather than chance events.

530 # Data availability

531 The algorithm used is freely available. Specific data used in the case studies are explained and

532 accounted for in Part II.

Author contributions

MvN designed method and paper, LT refined the empirical algorithm and handled the case study data and modeling for part II, and BL contributed statistical analysis; all contributed and approved the final manuscript

Acknowledgements

This research is part of the Forests, Trees and Agroforestry research program of the CGIAR. Several colleagues contributed to the development and early tests of the F_p method. Thanks are due to Eike Luedeling, Sonya Dewi, Sampurno Bruijnzeel and two anonymous reviewers for comments on an earlier version of the manuscript.

References

Alila, Y., Kura, P.K., Schnorbus, M., and Hudson, R.: Forests and floods: A new paradigm sheds light on age-old controversies, Water Resour. Res., 45, W08416, 2009.

Andréassian, V.: Waters and forests: from historical controversy to scientific debate, Journal of Hydrology, 291, 1–27, 2004.

Baldassarre, G.D., Kooy, M., Kemerink, J.S., and Brandimarte, L.: Towards understanding the dynamic behaviour of floodplains as human-water systems, Hydrology and Earth System Sciences, 17(8), 3235-3244, 2013.

Bardossy, A. and Plate, E.J.: Modeling daily rainfall using a semi-Markov representation of circulation pattern occurrence, Journal of Hydrology, 122(1), 33-47, 1991.

Band, L.E., Patterson, P., Nemani, R., and Running, S.W.: Forest ecosystem processes at the watershed scale: incorporating hillslope hydrology, Agricultural and Forest Meteorology, 63(1-2), 93-126, 1993.

Barnes, B.S.: The structure of discharge-recession curves, Eos, Transactions American Geophysical Union, 20(4), 721-725, 1939.

Beck, H. E., Bruijnzeel, L. A., Van Dijk, A. I. J. M., McVicar, T. R., Scatena, F. N., and Schellekens, J.: The impact of forest regeneration on streamflow in 12 mesoscale humid tropical catchments, Hydrology and Earth System Sciences ,17(7), 2613-2635, 2013.

Beven, K.J.: Rainfall-runoff modelling: the primer, John Wiley & Sons, 2011

561 Bishop, J. and Pagiola, S. (Eds.): Selling forest environmental services: market-based
562   mechanisms for conservation and development, Taylor & Francis, Abingdon (UK), 2012.

563 Bonell, M.: Progress in the understanding of runoff generation dynamics in forests, Journal of
564   Hydrology, 150(2), 217-275, 1993.

565 Bradshaw, C.J.A., Sodhi, N.S., Peh, K.S.H., and Brook, B.W.: Global evidence that
566   deforestation amplifies flood risk and severity in the developing world, Global Change
567   Biol, 13, 2379–2395, 2007.

568 Brauman, K.A., Daily, G.C., Duarte, T.K.E., and Mooney, H.A.: The nature and value of
569   ecosystem services: an overview highlighting hydrologic services, Annu. Rev. Environ.
570   Resour., 32, 67-98, 2007.

571 Bruijnzeel, L.A.: Hydrological functions of tropical forests: not seeing the soil for the trees,
572   Agr. Ecosyst. Environ., 104, 185–228, 2004.

573 Burt, T.P., Howden, N.J.K., McDonnell, J.J., Jones, J.A., and Hancock, G.R.: Seeing the
574   climate through the trees: observing climate and forestry impacts on streamflow using a
575   60-year record, Hydrological Processes, doi: 10.1002/hyp.10406, 2014.

576 Clark, W. C., Tomich, T. P., van Noordwijk, M., Guston, D., Catacutan, D., Dickson, N. M.,
577   and McNie, E.: Boundary work for sustainable development: natural resource
578   management at the Consultative Group on International Agricultural Research (CGIAR),
579   Proc. Nat. Acad. Sci., doi:10.1073/pnas.0900231108, 2011.

580 Delfs, J.O., Park, C.H., and Kolditz, O.: A sensitivity analysis of Hortonian flow, Advances in
581   Water Resources. 32(9), 1386-1395, 2009.

582 Evaristo, J., Jasechko, S., and McDonnell, J.J.: Global separation of plant transpiration from
583   groundwater and streamflow, Nature, 525(7567), 91-94, 2015.

584 Ghimire, C.P., Bruijnzeel, L.A., Lubczynski, M.W., and Bonell, M.: Negative trade-off
585   between changes in vegetation water use and infiltration recovery after reforesting
586   degraded pasture land in the Nepalese Lesser Himalaya, Hydrology and Earth System
587   Sciences, 18(12), 4933-4949, 2014.

588 Hrachowitz, M., Savenije, H.H.G., Blöschl, G., McDonnell, J.J., Sivapalan, M., Pomeroy,
589   J.W., Arheimer, B., Blume, T., Clark, M. P., Ehret, U., Fenicia, F., Freer, J E., Gelfan, A.,
590   Gupta, H.V., Hughes, D. A., Hut, R.W., Montanari, A., Pande, S., Tetzlaff, D., Troch,

P.A., Uhlenbrook, S., Wagener, T., Winsemius, H.C., Woods, R.A., Zehe, E., and Cudennec, C.: A decade of Predictions in Ungauged Basins (PUB)—a review, Hydrological sciences journal, 58(6), 1198-1255, 2013.

Ilstedt, U., Tobella, A.B., Bazié, H.R., Bayala, J., Verbeeten, E., Nyberg, G., Sanou, J., Benegas, L., Murdiyarso, D., Laudon, H., and Sheil, D.: Intermediate tree cover can maximize groundwater recharge in the seasonally dry tropics, Scientific reports, 6, 2016

Jones, P.G. and Thornton, P.K.: Spatial and temporal variability of rainfall related to a third-order Markov model, Agricultural and Forest Meteorology, 86(1), 127-138, 1997.

Jongman, B., Winsemius, H. C., Aerts, J. C., de Perez, E. C., van Aalst, M. K., Kron, W., and Ward, P. J.: Declining vulnerability to river floods and the global benefits of adaptation, In: Proceedings of the National Academy of Sciences, 112(18), E2271-E2280, 2015.

Joshi, L., Schalenbourg, W., Johansson, L., Khasanah, N., Stefanus, E., Fagerström, M.H., and van Noordwijk, M.,: Soil and water movement: combining local ecological knowledge with that of modellers when scaling up from plot to landscape level, In: van Noordwijk, M., Cadisch, G. and Ong, C.K. (Eds.) Belowground Interactions in Tropical Agroecosystems, CAB International, Wallingford (UK), 349-364, 2004.

Kirchhoff, C.J., Esselman, R., and Brown, D.: Boundary Organizations to Boundary Chains: Prospects for Advancing Climate Science Application, Climate Risk Management, doi:10.1016/j.crm.2015.04.001, 2015.

Lacombe, G. and McCartney, M.: Evaluating the flow regulating effects of ecosystems in the Mekong and Volta river basins, Colombo, Sri Lanka, International Water Management Institute (IWMI) Research Report 166,doi: 10.5337/2016.202, 2016.

Lacombe, G., Ribolzi, O., de Rouw, A., Pierret, A., Latsachak, K., Silvera, N., Pham Dinh, R., Orange, D., Janeau, J.-L., Soulileuth, B., Robain, H., Taccoen, A., Sengphaathith, P., Mouche, E., Sengtaheuanghoung, O., Tran Duc, T., and Valentin, C.: Afforestation by natural regeneration or by tree planting: Examples of opposite hydrological impacts evidenced by long-term field monitoring in the humid tropics, Hydrology and Earth System Sciences Discussions, 12, 12615-12648, 2015.

Leimona, B., Lusiana, B., van Noordwijk, M., Mulyoutami, E., Ekadinata, A., and Amaruzama, S.: Boundary work: knowledge co-production for negotiating payment for watershed services in Indonesia, Ecosystems Services, 15, 45–62, 2015.

Liu, W., Wei, X., Fan, H., Guo, X., Liu, Y., Zhang, M., and Li, Q.: Response of flow regimes to deforestation and reforestation in a rain-dominated large watershed of subtropical China, Hydrological Processes, 29, 5003-5015 , 2015.

Lusiana, B., van Noordwijk, M., Suyamto, D., Joshi, L., and Cadisch, G.: Users' perspectives on validity of a simulation model for natural resource management, International Journal of Agricultural Sustainability, 9(2), 364-378, 2011.

Ma, X., Xu, J. and van Noordwijk, M.: Sensitivity of streamflow from a Himalayan catchment to plausible changes in land-cover and climate, Hydrological Processes, 24, 1379–1390, 2010.

Ma, X., Lu, X., van Noordwijk, M., Li, J.T., and Xu, J.C.: Attribution of climate change, vegetation restoration, and engineering measures to the reduction of suspended sediment in the Kejie catchment, southwest China, Hydrol. Earth Syst. Sci., 18, 1979–1994, 2014.

Maidment, D.R.: Handbook of hydrology, McGraw-Hill Inc., 1992.

Malmer, A., Murdiyarso, D., Bruijnzeel L.A., and Ilstedt, U.: Carbon sequestration in tropical forests and water: a critical look at the basis for commonly used generalizations, Global Change Biology, 16(2), 599-604, 2010.

McCluney, K.E., Poff, N.L., Palmer, M.A., Thorp, J.H., Poole, G.C., Williams, B.S., Williams, M.R., and Baron, J.S.: Riverine macrosystems ecology: sensitivity, resistance, and resilience of whole river basins with human alterations, Frontiers in Ecology and the Environment, 12(1), 48-58, 2014.

Milly, P.C.D., Wetherald, R., Dunne, K.A., and Delworth, T.L.: Increasing risk of great floods in a changing climate, Nature, 415(6871), 514-517, 2002.

Palmer, M.A.: Reforming watershed restoration: science in need of application and applications in need of science, Estuaries and coasts, 32(1), 1-17, 2009.

Rahayu, S., Widodo, R.H., van Noordwijk, M., Suryadi, I., and Verbist, B.: Water monitoring in watersheds. Bogor, Indonesia, World Agroforestry Centre (ICRAF) SEA Regional Program,, 2013

650   Ranieri, S.B.L., Stirzaker, R., Suprayogo, D., Purwanto, E., de Willigen, P., and van
651   Noordwijk, M.: Managing movements of water, solutes and soil: from plot to landscape
652   scale. In: van Noordwijk, M., Cadisch, G. and Ong, C.K. (Eds.) Belowground
653   Interactions in Tropical Agroecosystems, CAB International, Wallingford (UK), 329-347,
654   2004.

655   Rodríguez-Iturbe, I. and Rinaldo, A.: Fractal river basins: chance and self-organization,
656   Cambridge University Press, Cambridge, 2001.

657   Richter, B.D., Mathews, R., Harrison, D.L., and Wigington, R.: Ecologically sustainable
658   water management: managing river flows for ecological integrity, Ecological
659   applications, 13(1), 206-224, 2003.

660   Rudel, T. K., Coomes, O. T., Moran, E., Achard, F., Angelsen, A., Xu, J., and Lambin, E.:
661   Forest transitions: towards a global understanding of land use change, Global
662   Environmental Change, 15(1), 23-31, 2005.

663   Sumarga, E., Hein, L., Hooijer, A., and Vernimmen, R.: Hydrological and economic effects of
664   oil palm cultivation in Indonesian peatlands, Ecology and Society, 21(2), 2016.

665   Tallaksen, L.M.: A review of baseflow recession analysis, J Hydrol, 165, 349-370, 1995.

666   Tan-Soo, J.S., Adnan, N., Ahmad, I., Pattanayak, S.K., and Vincent, J.R.: Econometric
667   Evidence on Forest Ecosystem Services: Deforestation and Flooding in
668   Malaysia. Environmental and Resource Economics, on-line:
669   http://link.springer.com/article/10.1007/s10640-014-9834-4, 2014.

670   van de Giesen, N.C., Stomph, T.J., and De Ridder, N.: Scale effects of Hortonian overland
671   flow and rainfall–runoff dynamics in a West African catena landscape, Hydrological
672   Processes, 14,165-175, 2000.

673   van Dijk, A.I., van Noordwijk, M., Calder, I.R., Bruijnzeel, L.A., Schellekens, J., and
674   Chappell, N.A.: Forest-flood relation still tenuous – comment on 'Global evidence that
675   deforestation amplifies flood risk and severity in the developing world', Global Change
676   Biology, 15, 110-115, 2009.

677   van Noordwijk, M., van Roode, M., McCallie, E.L., and Lusiana, B.: Erosion and
678   sedimentation as multiscale, fractal processes: implications for models, experiments and
679   the real world, In: F. Penning de Vries, F. Agus and J. Kerr (Eds.) Soil Erosion at Multiple

Scales, Principles and Methods for Assessing Causes and Impacts.. CAB International, Wallingford, 223-253, 1998.

van Noordwijk, M., Agus, F., Verbist, B., Hairiah, K., and Tomich, T.P.: Managing Watershed Services, In: Scherr, S.J. and McNeely, J.A. (Eds) Ecoagriculture Landscapes. Farming with Nature: The Science and Practice of Ecoagriculture, Island Press, Washington DC, 191 – 212, 2007.

van Noordwijk, M., Widodo, R.H., Farida, A., Suyamto, D., Lusiana, B., Tanika, L., and Khasanah, N.: GenRiver and FlowPer: Generic River and Flow Persistence Models. User Manual Version 2.0. Bogor, Indonesia, World Agroforestry Centre (ICRAF) Southeast Asia Regional Program, 2011.

van Noordwijk, M., Leimona, B., Jindal, R., Villamor, G.B., Vardhan, M., Namirembe, S., Catacutan, D., Kerr, J., Minang, P.A., and Tomich, T.P.: Payments for Environmental Services: evolution towards efficient and fair incentives for multifunctional landscapes, Annu. Rev. Environ. Resour., 37, 389-420, 2012.

van Noordwijk, M., Lusiana, B., Leimona, B., Dewi, S., and Wulandari, D.: Negotiation-support toolkit for learning landscapes, Bogor, Indonesia, World Agroforestry Centre (ICRAF) Southeast Asia Regional Program, 2013.

van Noordwijk, M., Leimona, B., Xing, M., Tanika, L., Namirembe, S., and Suprayogo, D.,: Water-focused landscape management. Climate-Smart Landscapes: Multifunctionality In Practice. eds Minang PA et al.. Nairobi, Kenya, World Agroforestry Centre (ICRAF), 179-192, 2015a.

van Noordwijk, M., Bruijnzeel, S., Ellison, D., Sheil, D., Morris, C., Gutierrez, V., Cohen, J., Sullivan, C., Verbist, B., and Muys, B.: Ecological rainfall infrastructure: investment in trees for sustainable development, ASB Brief no 47. Nairobi. ASB Partnership for the Tropical Forest Margins, 2015b.

Verbist, B., Poesen, J., van Noordwijk, M. Widianto, Suprayogo, D., Agus, F., and Deckers, J.: Factors affecting soil loss at plot scale and sediment yield at catchment scale in a tropical volcanic agroforestry landscape, Catena, 80, 34-46, 2010.

Weiler, M. and McDonnell, J.: Virtual experiments: a new approach for improving process conceptualization in hillslope hydrology, Journal of Hydrology, 285(1), 3-18, 2004

710   Winsemius, H.C., van   Beek, L.P.H., Jongman, B., Ward, P.J., and   Bouwman, A.:   A

711   framework for global river flood risk assessments, Hydrol Earth Syst Sci, 17,1871–1892,

712   2013.

713   Yen, H., White, M.J., Jeong, J., Arabi, M. and Arnold, J.G.: Evaluation of alternative surface

714   runoff accounting procedures using the SWAT model, International Journal of

715   Agricultural and Biological Engineering, 8(3), 54-68, 2015.

716   Zhou, G., Wei, X., Luo, Y., Zhang, M., Li, Y., Qiao, Y., Liu, H., and Wang, C.: Forest

717   recovery and river discharge at the regional scale of Guangdong Province, China, Water

718   Resources Research, 46(9), W09503, doi:10.1029/2009WR00829, 2010.

719
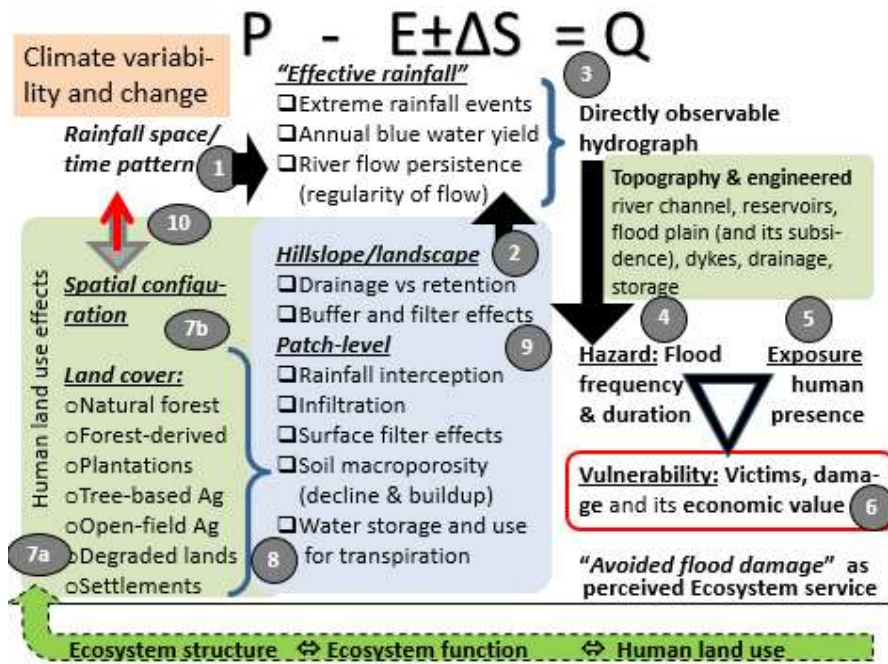
721 Figure 1. Steps in a causal pathway that relates rainfall (1) via watershed conditions (2) to the

722   pattern of river flow described in a hydrograph (3), which can get modified by the

723   conditions along the river channel into a hazard of flood frequency and duration (4); jointly

724   with exposure (being in the wrong place at critical times; 5) and vulnerability (6)

725   determines flood damage; in avoiding flood damage, the condition in the watershed with its

726   landcover and spatial configuration (7) influences the patchlevel water partitioning over

727   overlandflow and infitration (8) and hillslope level further influences on flow pathwatys (9)

728

729
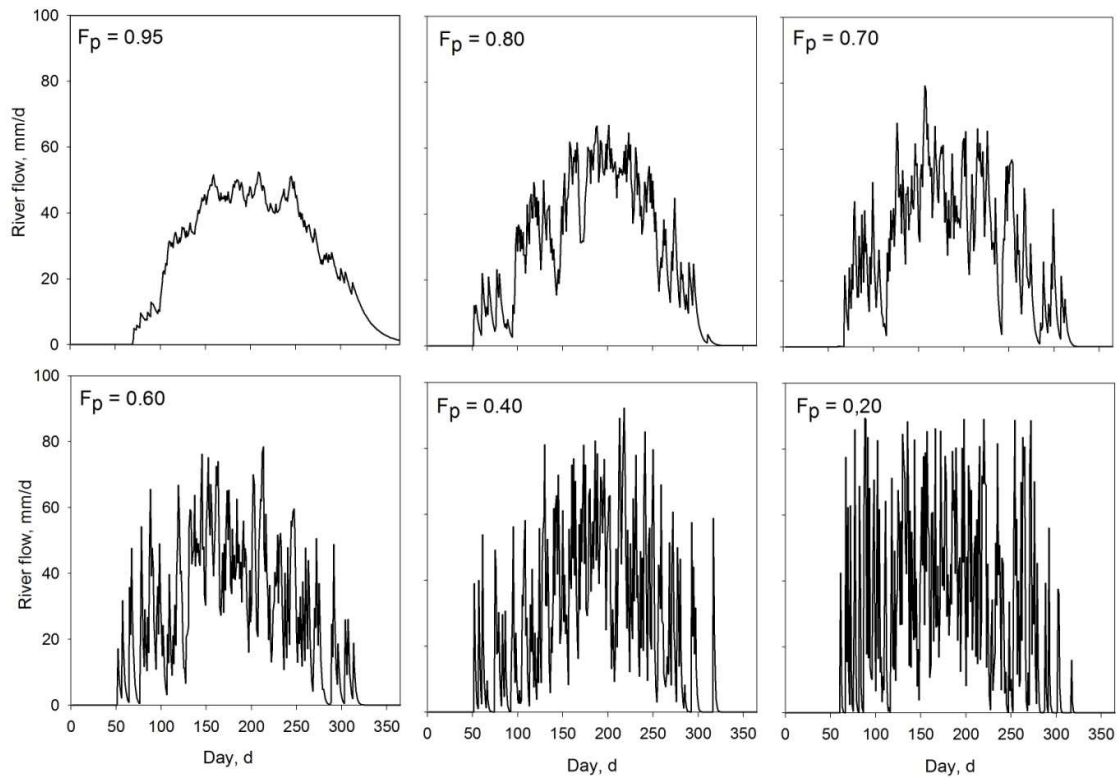
730

731 Figure 2. Example of daily river flow for a unimodal rainfall regime with clear dry season, in

732 response to change in the flow persistence parameter F_p

733
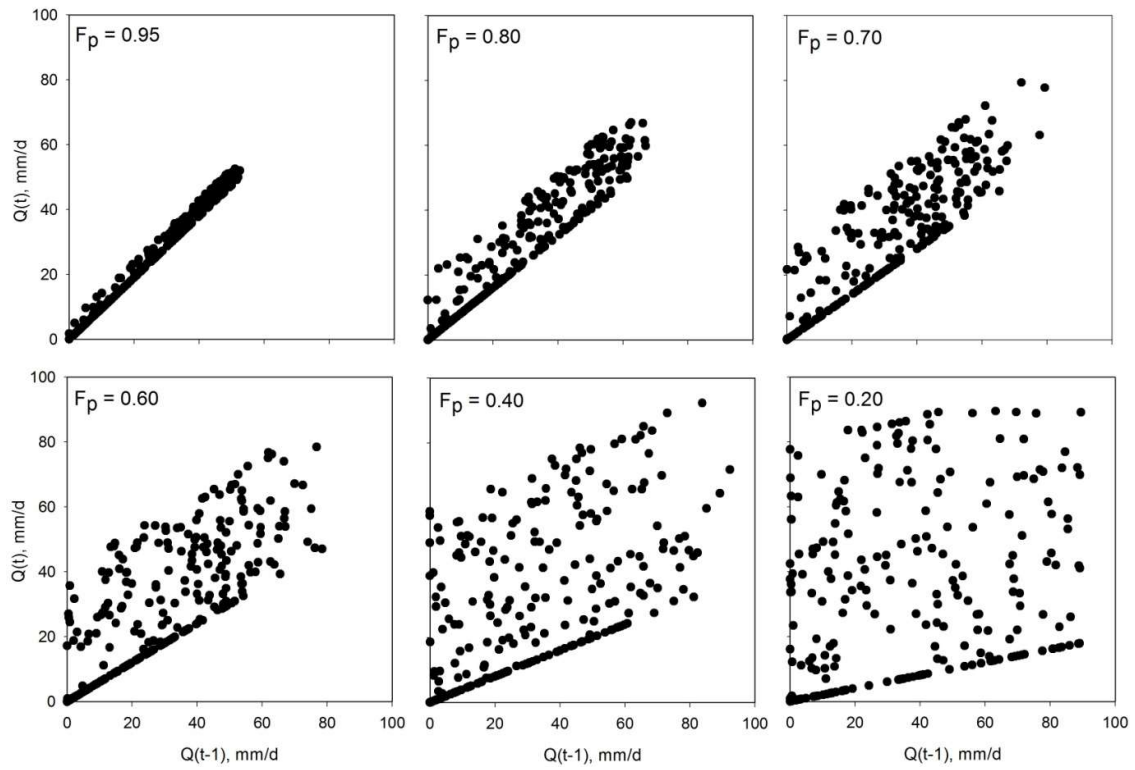
734

735   Figure 3. Biplots of Q(t) versus Q(t-1) for the same simulations as figure 2

736
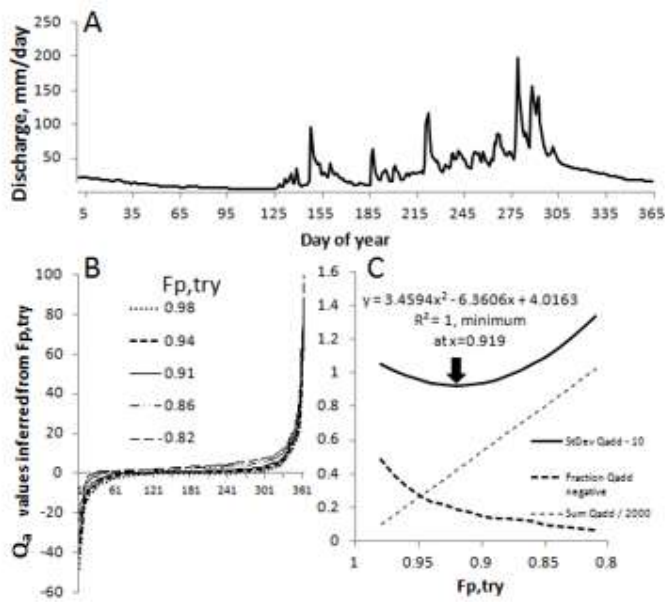
737

738   Figure 4. Example of the derivation of best fitting $F_{p,try}$ value for an example hydrograph (A)

739   on the basis of the inferred Q_a distribution (cumulative frequency in B), and three

740   properties of this distribution (C): its sum, frequency of negative values and standard

741   deviation; the $F_{p,try}$ minimum of the latter is derived from the parameters of a fitted

742   quadratic equation

743
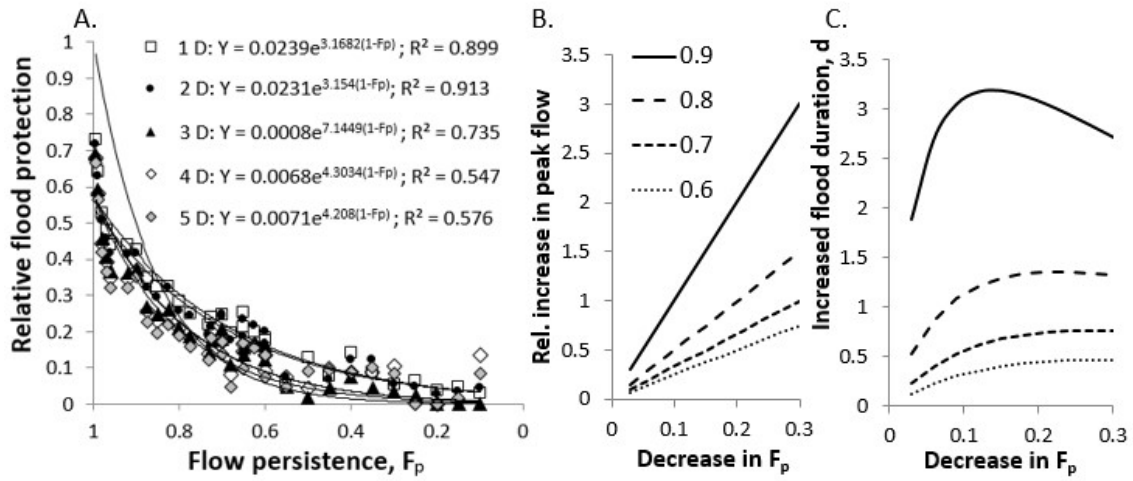
744
745
746   Figure 5. A. Effects of flow persistence on the relative flood protection (decrease in maximum
747   flow measured over a 1 – 5 d period relative to a case with $F_p = 0$ (a few small negative
748   points were replaced by small positive values to allow the exponential fit); B and C. effects
749   of a decrease in flow persistence on the volume of water involved in peak flows (B;
750   relative to the volume at F_p is 0.6 – 0.9) and in the duration (in d) of floods (C)
751

Flood risk reduction and flow buffering as ecosystem services: II. Land use and rainfall intensity effects in Southeast Asia

Meine van Noordwijk[1,2], Lisa Tanika[1], Betha Lusiana[1] [1]{World Agroforestry Centre (ICRAF), SE Asia program, Bogor, Indonesia}

 [2]{Wageningen University, Plant Production Systems, Wageningen, the Netherlands}

Correspondence to: Meine van Noordwijk (m.vannoordwijk@cgiar.org)

Abstract

The way watersheds with their vegetation, soils, geomorphology and geological substrate as well as riparian wetlands buffer the temporal pattern of riverflow relative to the temporal pattern of rainfall is an important ecosystem service that requires quantification. Part of it is inherent to its geology and climate, but another part is also responding to human use and misuse of the landscape, and can be part of management feedback loops if salient, credible and legitimate indicators can be found and used. The benefits to humans of reduced exposure to floods and increased riverflow in periods without rain are logically linked through the water balance. Dissecting the anthropogenic change from exogenous variability (e.g. the specific time-space pattern of rainfall during an observation period) is relevant for designing and monitoring of watershed management interventions. Part I introduced the concept of flow persistence, key to a parsimonious recursive model of river flow. It also discussed the operational derivation of the F_p parameter. Here we compare F_p estimates from four meso-scale watersheds in Indonesia (Cidanau, Way Besai, and Bialo) and Thailand (Mae Chaem), with varying climate, geology and land cover history, at a decadal time scale. The likely response in each of these four to variation in rainfall properties (incl. the maximum hourly rainfall intensity) and land cover (comparing scenarios with either more or less forest and tree cover than the current situation) was explored through a basic daily waterbalance model, GenRiver. This model was calibrated for each site on existing data, before being used to explore alternative land cover and rainfall parameter settings. In both data and model runs, the wet-season (3-monthly) F_p values were consistently lower than dry-season values for all four sites. Across the four catchments Fp values decreased with increasing annual rainfall, but specific

782   aspects of watersheds, such as the riparian swamp (peat soils) in Cidanau reduced

783   effects of land use change in the upper watershed. Increasing the mean rainfall

784   intensity (at constant monthly totals for rainfall) around the values considered typical

785   for each landscape was predicted to decrease F_p values by between 0.047 (Bialo) and

786   0.261 (Mae Chaem). In three of the four watersheds the effects on F_p of shifts in mean

787   rainfall intensity were 2.2 to 3.1 times larger than the land use change scenarios, but in

788   Bialo its relative effect was only 58%. Apparently, the sensitivity to changes in land

789   use change plus changes in rainfall intensity depends on other characteristics of the

790   watersheds, and generalizations made on the basis of one or two case studies may not

791   hold, even within the same climatic zone. A wet-season F_p value above 0.7 was

792   achievable in forest-agroforestry mosaic case studies. Interannual variability in F_p was

793   found to be large relative to effects of land cover change. The sensitivity in the model

794   of Hortonian overland flow to variations in rainfall intensity can account for the

795   interannual variability. Multiple (5-10) years of paired-plot data would generally be

796   needed to reject no-change null-hypotheses on the effects of land use change

797   (degradation and restoration). While empirical evidence of such effects at scale is

798   understandably scarce, F_p trends over time serve as a holistic scale-dependent

799   performance indicator of degrading/recovering watershed health and can be tested for

800   acceptability and acceptance in a wider socio-ecological context.

801   **Introduction**

802   Inherent properties (geology, geomorphology) interact with climate and human modification

803   of vegetation, soils, drainage and riparian wetlands in the degree of buffering that watersheds

804   provide (Andréassian 2004; Bruijnzeel, 2004). Buffering of riverflow relative to the space-

805   time dynamics of rainfall is an ecosystem service, reducing the exposure of people living on

806   geomorphological floodplains to high-flow events, and increasing predictability and river

807   flow in dry periods (Joshi et al., 2004; Leimona et al., 2015; Part I). In the absence of any

808   vegetation and with a sealed surface, riverflow will directly respond to the spatial distribution

809   of rainfall, with only the travel time to any point of specific interest influencing the remporal

810   pattern of river flow. Any persistence or predictability of river flow in such a situation will

811   reflect temporal autocorrelation of rainfall, beyond statistical predictability in seasonal rainfall

812   patterns. On the other side of the spectrum, riverflow can be constant every day, beyond the

813   theoretical condition of constant rainfall, in a watershed that provides perfect buffering, by

814 passing all water through groundwater pools that have sufficient storage capacity at any time

815 during the year. Both infiltration-limited (Hortonian) and saturation-induced use of more

816 rapid flow pathways (inter and overland flows) will reduce the flow persistence and make it,

817 at least in part dependent on rainfall events. Separating the effects of land cover (land use),

818 engineering and rainfall on the actual flow patterns of rivers remains a considerable challenge

819 (Ma et al., 2014; Verbist et al., 2019). It requires data, models and concepts that can serve as

820 effective boundary object in communication with stakeholders (Leimona et al. 2015; van

821 Noordwijk et al. 2012). There is a long tradition in using forest cover as such a boundary

822 object, but there is only a small amount of evidence supporting this (Tan-Soo et al., 2014; van

823 Dijk et al., 2009; van Noordwijk et al. 2015a).

824 In part I, we introduced a flow persistence parameter (F_p) that links the two, asymmetrical

825 aspects of flow dynamics: translating rainfall excess into river flow, and gradually releasing

826 water stored in the landscape. Here, in part II we will apply the F_p algorithm to river flow

827 data for a number of contrasting meso-scale watersheds in Southeast Asia. These were

828 selected to represent variation in rainfall and land cover, and test the internal consistency of

829 results based on historical data: two located in the humid and one in the subhumid tropics of

830 Indonesia, and one in the unimodal subhumid tropics of northern Thailand.

831 After exploring the patterns of variation in F_p estimates derived from river flow records, we

832 will quantify the sensitivity of the F_p metric to variations in rainfall intensity, and its response,

833 on a longer timescale to land cover change. To do so, we will use a model that uses basic

834 water balance concepts: rainfall interception, infiltration, water use by vegetation, overland

835 flow, interflow and groundwater release, to a spatially structured watershed where travel time

836 from subwatersheds to any point of interest modifies the predicted riverflow. In the specific

837 model used land cover effects on soil conditions, interception and seasonal water use have

838 been included. After testing whether F_p values derived from model outputs match those based

839 on empirical data where these exist, we rely on the basic logic of the model to make inference

840 on the relative importance of modifying rainfall and land cover inputs. With the resulting

841 temporal variation in calculated F_p values, we consider time frame at which observed shifts in

842 F_p can be attributed to factors other than chance (that means: null-hypotheses of random

843 effects can be rejected with accepted chance of Type I errors).

844 **2. Methods**

845 **2.1 GenRiver model for effects of land cover on river flow**

846   The GenRiver model (van Noordwijk et al., 2011) is based on a simple water balance concept

847   with a daily timestep and a flexible spatial subdivision of a watershed that influences the

848   routing of water and employs spatially explicit rainfall. At patchlevel, vegetation influences

849   interception, retention for subsequent evaporation and delayed transfer to the soil surface, as

850   well as the seasonal demand for water. Vegetation (land cover) also influences soil porosity

851   and infiltration, modifying the inherent soil properties. Water in the root zone is modelled

852   separately for each land cover within a subcatchment, the groundwater stock is modelled at

853   subcatchment level. The spatial structure of a watershed and the routing of surface flows

854   influences the timedelays to any specified point of interest, which normally includes the

855   outflow of the catchment. Land-cover change scenarios are interpolated annually between

856   time-series (measured or modelled) data. The model may use measured rainfall data, or use a

857   rainfall generator that involves Markov chain temporal autocorrelation (rain persistence). As

858   our data sources are mostly restricted to daily rainfall measurements and the infiltration model

859   compares instantaneous rainfall to infiltration capacity, a stochastic rainfall intensity was

860   applied at subcatchment level, driven by the mean as parameter and a standard deviation for a

861   normal distribution (truncated at 3 standard deviations from the mean) proportional to it via a

862   coefficient of variation as parameter. For the Mae Chaem site in N Thailand data by Dairaku

863   et al. (2004) suggested a mean of less than 3 mm/hr. For the three sites in Indonesia we used

864   30 mm/hr, based on Kusumastuti et al. (2016). Appendix 1 provides further detail on the

865   GenRiver model. The model itself, a manual and application case studies are freely available

866   (http://www.worldagroforestry.org/output/genriver-genetic-river-model-river-flow;van

867   Noordwijk et al., 2011).

2.2 Empirical data-sets, model calibration

869   Table 1 and Fig.1 provides summary characteristics and the location of river flow data are

870   used in four meso-scale watersheds for testing the F_p algorithm and application of the

871   GenRiver model. Figure 1 includes a water tower category in the agro-ecological zones; this

872   is defined on the basis of a ratio of precipitation and potential evapotranspiration of more than

873   0.65, and a product of that ratio and relative elevation exceeding 0.277.

874   ⇨ Table 1
875   ⇨ Fig. 1

876   As major parameters for the GenRiver model were not independently measured for the

877   respective watersheds, we tuned (calibrated) the model by modifying paraemeters within a

878   predetrimined plausible range, and used correspondence with measured hydrograph as test

879 criterion (Kobolt et al. 2008). We used the Nash-Sutcliff Efficiency (NSE) parameter (target

880 above 0.5) and bias (less than 25%) as test criteria and targets. Meeting these performance

881 targets (Moriasi et al., 2007), we accepted the adjusted models as basis for describing current

882 conditions and exploring model sensitivity. The main site-specific parameter values are listed

883 in Table 2 and (generic) land-cover specific default parameters in Table 3.

884 ⇨ Table 2
885 ⇨ Table 3

886 Table 4 describes the six scenarios of land-use change that were evaluated in terms of their

887 hydrological impacts. Further description on the associated land cover distribution for each

888 scenario in the four different watersheds is depicted in Appendix 2.

889 ⇨ Table 4

890 **2.3 Bootstrapping to estimate the minimum observation**

891 The bootstrap methods (Efron and Tibshirani, 1986) is a resampling methods that is

892 commonly used to generate 'surrogate population' for the purpose of approximating the

893 sampling distribution of a statistic. In this study, the bootstrap approach was used to estimate

894 the minimum number of observation (or yearly data) required for a pair-wise comparison test

895 between two time-series of stream flow or discharge data (representing two scenarios of land

896 use distributions) to be distinguishable from a null-hypothesis of no effect. The pair-wise

897 comparison test used was Kolmogorov-Smirnov test that is commonly used to test the

898 distribution of discharge data (Zhang eta al, 2006). We built a simple macro in R (R Core

899 Team, 2015) that entails the following steps:

900 (i) Bootstrap or resample with replacement 1000 times from both time-series discharge
901   data with sample size n;

902 (ii) Apply the Kolmogorov-Smirnov test to each of the 1000 generated pair-wise
903   discharge data, and record the P-value;

904 (iii) Perform (i) and (ii) for different size of n, ranging from 5 to 50.

905 (iv) Tabulate the p-value from the different sample size n, and determine the value of n
906   when the p-value reached equal to or less than 0.025 (or equal to the significance level
907   of 5%). The associated n represents the minimum number of observations required.

908 Appendix 3 provides an example of the macro in R used for this analysis.

3. Results

3.1 Empirical data of flow persistence as basis for model parameterization

Inter-annual variability of F_p estimates derived for the four catchments (Fig. 2) was of the order of 0.1 units, while the intra-annual variability between dry and rainy seasons was 0.1-0.2. For all for the years and locations, rainy season F_p values, with mixed flow pathways, were consistently below dry-season values, dominated by groundwater flows. If we can expect $F_{p,i}$ and $F_{p,o}$ (see equation 8 in part I) to be approximately 0.5 and 0, this difference between wet and dry periods implies a 40% contribution of interflow in the wet season, a 20% contribution of overland flow or any combination of the two effects.

Overall the estimates from modeled and observed data are related with 16% deviating more than 0.1 and 3% more than 0.15 (Fig. 3). As the Moriasi et al. (2007) performance criteria for the hydrographs were met by the calibrated models for each site, we tentatively accept the model to be a basis for sensitivity study of F_p to modifications to land cover and/or rainfall

⇨ Fig. 2
⇨ Fig. 3

3.2 Comparing F_p effects of rainfall intensity and land cover change

A direct comparison of model sensitivity to changes in mean rainfall intensity and land use change scenarios is provided in Fig. 4. Varying the mean rainfall intensity over a factor 7 shifted the F_p value by only 0.047 and 0.059 in the case of Bialo and Cidanau, respectively, but by 0.128 in Way Besaiand 0.261 in Mae Chaem (Fig. 4A). The impact of the land use change scenarios on F_p was smallest in Cidanau (0.026), intermediate in Way Besai (0.048) and relatively large in Bialo and Mae Chaem, at 0.080 and 0.084, respectively (Fig. 4B). The order of F_p across the land use change scenarios was mostly consistent between the watersheds, but the contrast between the ReFor and NatFor scenario was largest in Mae Chaem and smallest in Way Besai. In Cidanau, Way Besai and Mae Chaem, variations in rainfall were 2.2 to 3.1 times more effective than land use change in shifting F_p, in Bialo its relative effect was only 58%. Apparently, the sensitivity to changes in land use change plus changes in rainfall intensity depends on other characteristics of the watersheds, and generalizations made on the basis of one or two dace studies may not hold, even within the same climatic zone.

⇨ Fig. 4

3.3 Further analysis of F_p effects for scenarios of land cover change

Among the four watersheds there is consistency in that the 'forest' scenario has the highest, and the 'degraded lands' the lowest F_p value (Fig. 5), but there are remarkable differences as well: in Cidanau the interannual variation in F_p is clearly larger than land cover effects, while in the Way Besai the spread in land use scenarios is larger than interannual variability. In Cidanau a peat swamp between most of the catchment and measuring point buffers most of landcover related variation in flow, but not the interannual variability. Considering the frequency distributions of F_p values over a 20 year period, we see one watershed (Way Besai) where the forest stands out from all others, and one (Bialo) where the degraded lands are separate from the others. Given the degree of overlap of the frequency distributions, it is clear that multiple years of empirical observations will be needed before a change can be affirmed.

Figure 4 shows the frequency distributions of expected effect sizes on F_p of a comparison of any land cover with either forest or degraded lands. Table 5 translates this information to the number of years that a paired plot (in the absence of measurement error) would have to be maintained to reject a null-hypothesis of no effect, at p=0.05. As the frequency distributions of F_p differences of paired catchments do not match a normal distribution, a Kolmorov-Smirnov test can be used to assess the probability that a no-difference null hypothesis can yield the difference found. By bootstrapping within the years where simulations supported by observed rainfall data exist, we found for the Way Besai catchment, for example, that 20 years of data would be needed to assert (at P = 0.05) that the ReFor scenario differs from AgFor, and 16 years that it differs from Actual and 11 years that it differs from Degrade. In practice, that means that empirical evidence that survives statistical tests will not emerge, even though effects on watershed health are real.

⇨ Fig. 5
⇨ Table 5

At process-level the increase in 'overland flow' in response to soil compaction due to land cover change has a clear and statistically significant relationship with decreasing F_p values in all catchments (Fig 6), but both year-to-year variation within a catchment and differences between catchments influence the results as well, leading to considerable spread in the biplot. Contrary to expectations, the disappearance of 'interflow' by soil compaction is not reflected in measurable change in F_p value. The temporal difference between overland and interflow (one or a few days) gets easily blurred in the river response that integrates over multiple streams with variation in delivery times; the difference between overland- or interflow and baseflow is much more pronounced. Apparently, according to our model, the high

974 macroporosity of forest soils that allows interflow and may be the 'sponge' effect attributed to
975 forest, delays delivery to rivers by one or a few days, with little effect on the flow volumes at
976 locations downstream where flow of multiple days accumulates. The difference between
977 overland- or interflow and baseflow in time-to-river of rainfall peaks is much more
978 pronounced..

979 ⇨ Fig. 6

980 Tree cover has two contradicting effects on baseflow: it reduces the surplus of rainfall over
981 evapotranspiration (annual water yield) by increased evapotranspiration (especially where
982 evergreen trees are involved), but it potentially increases soil macroporosity that supports
983 infiltration and interflow, with relatively little effect on waterholding capacity measured as
984 'field capacity' (after runoff and interflow have removed excess water). Fig. 7 shows that the
985 total volume of baseflow differs more between sites and their rainfall pattern than it varies
986 with tree cover. Between years total evapotranspiration and baseflow totals are positively
987 correlated (see supplementary information), but for a given rainfall there is a tradeoff. Overall
988 these results support the conclusion that generic effects of deforestation on decreased flow
989 persistence, and of (agro)/(re)-forestation on increased flow persistence are small relative to
990 interannual variability due to specific rainfall patterns, and that it will be hard for any
991 empirical data process to pick-up such effects, even if they are qualitatively aligned with valid
992 process-based models.

993 ⇨ Fig. 7

994 **4. Discussion**

995 In the discussion of Part I the credibility questions on replicability of the F_p metric and its
996 sensitivity to details of rainfall pattern versus land cover as potential causes of variation were
997 seen as requiring case studies in a range of contexts. Although the four case studies in
998 Southeast Asia presented here cannot be claimed to represent the global variation in
999 catchment behaviour (with absence of a snowpack and its dynamics as an obvious element of
1000 flow buffering not included), the diversity of responses among these four allready point to
1001 challenges for any generic interpretation of the degree of flow persistence that can be
1002 achieved under natural forest cover, as well as its response to land cover change.

1003 The empirical data summarized here for (sub)humid tropical sites in Indonesia and Thailand
1004 show that values of F_p above 0.9 are scarce in the case studies provided, but values above 0.8
1005 were found, or inferred by the model, for forested landscapes. Agroforestry landscapes

1006   generally presented F_p values above 0.7, while open-field agriculture or degraded soils led to

1007 F_p values of 0.5 or lower. Due to differences in local context, it may not be feasible to relate

1008   typical F_p values to the overall condition of a watershed, but temporal change in F_p can

1009   indicate degradation or restoration if a location-specific reference can be found. The

1010   difference between wet and dry season F_p can be further explored in this context. The dry

1011   season F_p value primarily reflects the underlying geology, with potential modification by

1012   engineering and operating rules of reservoirs, the wet season F_p is generally lower due to

1013   partial shifts to overland and interflow pathways. Where further uncertainty is introduced by

1014   the use of modeled rather than measured river flow, the lack of fit of models similar to the

1015   ones we used here would mean that scenario results are indicative of directions of change

1016   rather than a precision tool for fine-tuning combinations of engineering and land cover change

1017   as part of integrated watershed management.

1018   The differences in relative response of the watersheds to changes in mean rainfall intensity

1019   and land cover change, suggest that generalizations derived from one or a few case studies are

1020   to be interpreted cautiously. If land cover change would influence details of the rainfall

1021   generation process (arrow 10 in Figure 1 of part I; e.g. through release of ice-nucleating

1022   bacteria Morris et al., 2014; van Noordwijk et al., 2015b) this can easily dominate over effects

1023   via interception, transpiration and soil changes.

1024   Our results indicate an intra-annual variability of F_p values between wet and dry seasons of

1025   around 0.2 in the case studies, while interannual variability in either annual or seasonal F_p was

1026   generally in the 0.1 range. The difference between observed and simulated flow data as basis

1027   for F_p calculations was mostly less than 0.1. With current methods, it seems that effects of

1028   land cover change on flow persistence that shift the F_p value by about 0.1 are the limit of what

1029   can be asserted from empirical data (with shifts of that order in a single year a warning sign

1030   rather than a firmly established change). When derived from observed river flow data F_p is

1031   suitable for monitoring change (degradation, restoration) and can be a serious candidate for

1032   monitoring performance in outcome-based ecosystem service management contracts.

1033   In view of our results the lack of robust evidence in the literature of effects of change in forest

1034   and tree cover on flood occurrence may not be a surprise; effects are subtle and most data sets

1035   contain considerable variability. Yet, such effects are consistent with current process and

1036   scaling knowledge of watersheds.

1037   **Data availability**

1038 Table 6 specifies the rainfall and river flow data we used for the four basins and specifies the

1039 links to detailed descriptions.

1040   ⇨ Table 6

Acknowledgements

1042 This research is part of the Forests, Trees and Agroforestry research program of the CGIAR.

1043 Several colleagues contributed to the development and early tests of the F_p method. Thanks

1044 are due to Thoha Zulkarnain for assistance with Figure 1 and to Eike Luedeling, Sonya Dewi,

1045 Sampurno Bruijnzeel and two anonymous reviewers for comments on an earlier version of the

1046 manuscript.

References

1048 Andréassian, V.: Waters and forests: from historical controversy to scientific debate, Journal
1049   of Hydrology, 291, 1–27, 2004.

1050 Bruijnzeel, L.A.: Hydrological functions of tropical forests: not seeing the soil for the trees,
1051   Agr. Ecosyst. Environ, 104, 185–228, 2004.

1052 Dairaku K., Emori, S., and Taikan, T.: Rainfall Amount, Intensity, Duration, and Frequency
1053   Relationships in the Mae Chaem Watershed in Southeast Asia, Journal of
1054   Hydrometeorology, 5, 458-470, 2004.

1055 Efron, B and Tibshirani, R.: Bootstrap Methods for Standard Errors, Confidence Intervals,
1056   and Other Measures of Statistical Accuracy. Statistical Science 1 (1): 54-75, 1986.

1057 Joshi, L., Schalenbourg, W., Johansson, L., Khasanah, N., Stefanus, E., Fagerström, M.H.,
1058   and van Noordwijk, M.,: Soil and water movement: combining local ecological
1059   knowledge with that of modellers when scaling up from plot to landscape level, In: van
1060   Noordwijk, M., Cadisch, G. and Ong, C.K. (Eds.) Belowground Interactions in Tropical
1061   Agroecosystems, CAB International, Wallingford (UK), 349-364, 2004.

1062 Kobold, M., Suselj, K., Polajnar, J., and Pogacnik, N.: Calibration Techniques Used For HBV
1063   Hydrological Model In Savinja Catchment,In: XXIVth Conference of the Danubian
1064   Countries On The Hydrological Forecasting And Hydrological Bases Of Water
1065   Management, 2008.

1066   Kusumastuti, D.I., Jokowinarno, D., van Rafi'i, C.H., and Yuniarti, F.: Analysis of rainfall
1067   characteristics for flood estimation in Way Awi watershed, Civil Engineering Dimension,
1068   18, 31-37, 2016

1069   Leimona, B., Lusiana, B., van Noordwijk, M., Mulyoutami, E., Ekadinata, A., and
1070   Amaruzama, S.: Boundary work: knowledge co-production for negotiating payment for
1071   watershed services in Indonesia, Ecosystems Services, 15, 45–62, 2015.

1072   Ma, X., Lu, X., van Noordwijk, M., Li, J.T., and Xu, J.C.: Attribution of climate change,
1073   vegetation restoration, and engineering measures to the reduction of suspended sediment
1074   in the Kejie catchment, southwest China, Hydrol. Earth Syst. Sci., 18, 1979–1994, 2014.

1075   Moriasi, D.N., Arnold, J.G., Van Liew, M.W., Bingner, R.L., Harmel, R.D., and Veith, T.L.:
1076   Model Evaluation Guidelines For Systematic Quantification Of Accuracy In Watershed
1077   Simulations, American Society of Agricultural and Biological Engineers, 20(3),885-900,
1078   2001

1079   Morris, C.E., Conen, F., Huffman, A., Phillips, V., Pöschl, U., and Sands, D.C.:
1080   Bioprecipitation: a feedback cycle linking Earth history, ecosystem dynamics and land use
1081   through biological ice nucleators in the atmosphere, Glob Change Biol, 20, 341-351.
1082   2014.

1083   R Core Team R: A language and environment for statistical computing. R Foundation for
1084   Statistical Computing, Vienna, Austria, URL http://www.R-project.org/, 2015

1085   Tan-Soo, J.S., Adnan, N., Ahmad, I., Pattanayak, S.K., and Vincent, J.R.: Econometric
1086   Evidence on Forest Ecosystem Services: Deforestation and Flooding in Malaysia.
1087   Environmental and Resource Economics, on-line:
1088   http://link.springer.com/article/10.1007/s10640-014-9834-4, 2014.

1089   van Dijk, A.I., van Noordwijk, M., Calder, I.R., Bruijnzeel, L.A., Schellekens, J., and
1090   Chappell, N.A.: Forest-flood relation still tenuous – comment on 'Global evidence that
1091   deforestation amplifies flood risk and severity in the developing world', Global Change
1092   Biology, 15, 110-115, 2009.

1093   van Noordwijk, M., Widodo, R.H., Farida, A., Suyamto, D., Lusiana, B., Tanika, L., and
1094   Khasanah, N.: GenRiver and FlowPer: Generic River and Flow Persistence Models. User
1095   Manual Version 2.0, Bogor, Indonesia, World Agroforestry Centre (ICRAF) Southeast
1096   Asia Regional Program, 2011.

1097 van Noordwijk, M., Leimona, B., Jindal, R., Villamor, G.B., Vardhan, M., Namirembe, S.,
1098   Catacutan, D., Kerr, J., Minang, P.A., and Tomich, T.P.: Payments for Environmental
1099   Services: evolution towards efficient and fair incentives for multifunctional landscapes,
1100   Annu. Rev. Environ. Resour., 37, 389-420, 2012.

1101 van Noordwijk, M., Leimona, B., Xing, M., Tanika, L., Namirembe, S., and Suprayogo, D.:
1102   Water-focused landscape management. Climate-Smart Landscapes: Multifunctionality In
1103   Practice, eds Minang PA et al.. Nairobi, Kenya: World Agroforestry Centre (ICRAF),
1104   179-192, 2015a.

1105 van Noordwijk, M., Bruijnzeel, S., Ellison, D., Sheil, D., Morris, C., Gutierrez, V., Cohen, J.,
1106   Sullivan, C., Verbist, B., and Muys, B.: Ecological rainfall infrastructure: investment in
1107   trees for sustainable development, ASB Brief no 47, Nairobi, ASB Partnership for the
1108   Tropical Forest Margins, 2015b.

1109 Verbist, B., Poesen, J., van Noordwijk, M. Widianto, Suprayogo, D., Agus, F., and Deckers,
1110   J.: Factors affecting soil loss at plot scale and sediment yield at catchment scale in a
1111   tropical volcanic agroforestry landscape, Catena, 80, 34-46, 2010.

1112 Zhang, Q., Liu, C., Xu, C., Xu, and Jiang T.: Observed trends of annual maximum water
1113   level and streamflow during past 130 years in the Yangtze River basin, China, Journal of
1114   Hydrology, 324, 255-265, 2006.
1115

1116   Table 1. Basic physiographic characteristics of the four study watersheds

Parameter	Bialo	Cidanau	Mae Chaem	Way Besai
Location	South Sulawesi, Indonesia	West Java, Indonesia	Northern Thailand	Lampung, Sumatera, Indonesia
Area (km^2)	111.7	241.6	3892	414.4
Elevation (m a.s.l.)	0 – 2874	30 – 1778	475-2560	720-1831
Flow pattern	Parallel	Parallel (with two main river flow that meet in the downstream area)	Parallel	Radial
Land cover type	Forest (13%) Agroforest (59%) Crops (22%) Others (6%)	Forest (20%) Agroforest (32%) Crops (33%) Others (11%) Swamp(4%)	Forest (evergreen, deciduous and pine) (84%) Crops (15%) Others (1%)	Forest (18%) Coffee (monoculture and multistrata) (64%) Crop and Holticulture (12%) Others (6%)
Mean annual rainfall, mm	1695	2573	1027	2474
Wet season	April – June	January - March	July - September	January - March
Dry season	July - September	July - September	January - March	July - September
Mean annual runoff, mm	947	917	259	1673
Major soils	Inceptisols	Inceptisols	Ultisols, Entisols	Andisols
% Natural forest	13	3.1 (forest and swamp forest)	84 (deciduous, evergreen, pine)	3.6

1117

1118   Table 2. Parameters of the GenRiver model used for the four site specific simulations (van

1119   Noordwijk et al., 2011 for definitions of terms; sequence of parameters follows the pathway

1120   of water)

Parameter	Definition	Unit	Bialo	Cidanau	Mae Chaem	Way Besai
RainIntensMean	Average rainfall intensity	mm hr^{-1}	30	30	3	30
RainIntensCoefVar	Coefficient of variation of rainfall intensity	mm hr^{-1}	0.8	0.3	0.5	0.3
RainInterceptDripRt	Max drip rate of intercepted rain	mm hr^{-1}	80	10	10	10
RainMaxIntDripDur	Max dripping duration of intercepted rain	Hr	0.8	0.5	0.5	0.5
InterceptEffectontrans	Rain interception effect on transpiration	-	0.35	0.8	0.3	0.8
MaxInfRate	Maximum infiltration capacity	mm d^{-1}	580	800	150	720
MaxInfSubsoil	Maximum infiltration sub soil capacity	mm d^{-1}	80	120	150	120
PerFracMultiplier	Daily soil water drainage as fraction of groundwater release fraction	-	0.35	0.13	0.1	0.1
MaxDynGrWatStore	Dynamic groundwater storage capacity	mm	100	100	300	300
GWReleaseFracVar	Groundwater release fraction, applied to all subcatchments	-	0.15	0.03	0.05	0.1
Tortuosity	Stream shape factor	-	0.4	0.4	0.6	0.45
Dispersal Factor	Drainage density	-	0.3	0.4	0.3	0.45
River Velocity	River flow velocity	m s^{-1}	0.4	0.7	0.35	0.5

1121

1122 Table 3. GenRiver defaults for land-use specific parameter values, used for all four
1123 watersheds (BD/BDref indicates the bulk density relative to that for an agricultural soil
1124 pedotransfer function; see van Noordwijk et al., 2011)

1125

Land cover Type	Potential interception (mm/d)	Relative drought threshold	BD/BDref
Forest[1]	3.0 - 4.0	0.4 - 0.5	0.8 - 1.1
Agroforestry[2]	2.0 - 3.0	0.5 - 0.6	0.95 - 1.05
Monoculture tree[3]	1.0	0.55	1.08
Annual crops	1.0 - 3.0	0.6 - 0.7	1.1 - 1.5
Horticulture	1.0	0.7	1.07
Rice field[4]	1.0 - 3.0	0.9	1.1 - 1.2
Settlement	0.05	0.01	1.3
Shrub and grass	2.0 - 3.0	0.6	1.0 - 1.07
Cleared land	1.0 - 1.5	0.3 - 0.4	1.1 - 1.2

1126 Note: 1. Forest: primary forest, secondary forest, swamp forest, evergreen forest, deciduous forest

1127   2. Agroforestry: mixed garden, coffee, cocoa, clove

1128   3. Monoculture : coffee

1129   4. Rice field: irrigation and rainfed

1130

1131   Table 4. Land use scenarios explored for four watersheds

Scenario	Description
NatFor	Full natural forest, hypothetical reference scenario
ReFor	Reforestation, replanting shrub, cleared land, grass land and some agricultural area with forest
AgFor	Agroforestry scenario, maintaining agroforestry areas and converting shrub, cleared land, grass land and some of agricultural area into agroforestry
Actual	Baseline scenario, based on the actual condition of land cover change during the modeled time period
Agric	Agriculture scenario, converting some of tree based plantations, cleared land, shrub and grass land into rice fields or dry land agriculture, while maintain existing forest
Degrading	No change in already degraded areas, while converting most of forest and agroforestry area into rice fields and dry land agriculture

1132

1133

Table 5. Number of years of observations required to estimate flow persistence to reject the null-hypothesis of 'no land use effect' at p-value = 0.05 using Kolmogorov-Smirnov test. The probability of the test statistic in the first significant number is provided between brackets and where the number of observations exceeds the time series available, results are given in *italics*

A. Natural Forest as reference

Way Besai (N=32)

	ReFor	AgFor	Actual	Agric
ReFor		20 (0.035)	16 (0.037)	13 (0.046)
AgFor			n.s.	n.s.
Actual				n.s.
Agric				
Degrading				

Bialo (N=18)

	ReFor	AgFor	Actual	Agric
ReFor		n.s.	n.s.	*37 (0.04)*
AgFor			n.s.	n.s.
Actual				n.s.
Agric				
Degrading				

Cidanau (N=20)

	ReFor	AgFor	Actual	Agric
ReFor		n.s.	n.s.	*32 (0.037)*
AgFor			n.s.	n.s.
Actual				n.s.
Agric				
Degrading				

Mae Chaem (N=15)

	ReFor	Actual	Agric	Degrade
ReFor		n.s.	*23 (0.049)*	*18 (0.050)*
Actual			*45 (0.037)*	*33 (0.041)*
Agric				*33 (0.041)*
Degrading				

B. **Degrading scenario as reference**

Way Besai (N=32)

	NatFor	ReFor	AgFor	Actual	Agric
NatFor		n.s.	17 (0.042)	13 (0.046)	7 (0.023)
ReFor			21 (0.037)	19 (0.026)	7 (0.023)
AgFor				n.s.	28 (0.046)
Actual					30 (0.029)
Agric					

Bialo (N=18)

	NatFor	ReFor	AgFor	Actual	Agric
NatFor		n.s.	n.s.	*41 (0.047)*	*19 (0.026)*
ReFor			n.s.	n.s.	*32 (0.037)*
AgFor				n.s.	n.s.
Actual					n.s.
Agric					

Cidanau (N=20)

	NatFor	ReFor	AgFor	Actual	Agric
NatFor		n.s.	n.s.	*33 (0.041)*	8 (0.034)
ReFor			n.s.	n.s.	15 (0.028)
AgFor				n.s.	n.s.
Actual					*25 (0.031)*
Agric					

Mae Chaem (N=15)

	NatFor	ReFor	Actual	Agric
NatFor		n.s.	25 (0.031)	12 (0.037)
ReFor			n.s.	*18 (0.050)*
Actual				*18 (0.050)*
Agric				

1139

1140 Table 6. Data availability

	Bialo	Cidanau	Mae Chaem	Way Besai
Rainfall data	1989-2009, Source: BWS Sulawesi[a] and PUSAIR[b]; Average rainfall data from the stations Moti, Bulo-bulo, Seka and Onto	1998-2008, source: BMKG[c]	1998-2002, source: WRD55, MTD22, RYP48, GMT13, WRD 52	1976-2007, Source: BMKG, PU[d] and PLN[e] (interpolation of 8 rainfall stations using Thiessen polygon)
River flow data	1993-2010, source; BWS Sulawesi and PUSAIR	2000-2009, source: KTI[f]	1954-2003, source: ICHARM[g]	1976-1998, source: PU and PUSAIR
Reference of detailed report	http://old.icraf.org/regions/southeast_asia/publications?do=view_pub_detail&pub_no=PP0343-14	http://worldagroforestry.org/regions/southeast_asia/publications?do=view_pub_detail&pub_no=PO0292-13	http://worldagroforestry.org/regions/southeast_asia/publications?do=view_pub_detail&pub_no=MN0048-11	http://worldagroforestry.org/regions/southeast_asia/publications?do=view_pub_detail&pub_no=MN0048-11

1141   Note:

1142   [a] BWS: Balai Wilayah Sungai (*Regional River Agency*)

1143   [b]PUSAIR: Pusat Litbang Sumber Daya Air (*Centre for Research and Development on Water*
1144   *Resources)*

1145   [c]BMKG: Badan Meteorologi Klimatologi dan Geofisika (*Agency on Meterology, Climatology*
1146   *and Geophysics*)

1147   [d]PU: Dinas Pekerjaan Unum *(Public Work Agency)*

1148   [e]PLN: Perusahaan Listrik Negara (*National Electric Company*)

1149   [f]KTI: Krakatau Tirta Industri, a private steel company

1150   [f]ICHARM: The International Centre for Water Hazard and Risk Management

1151
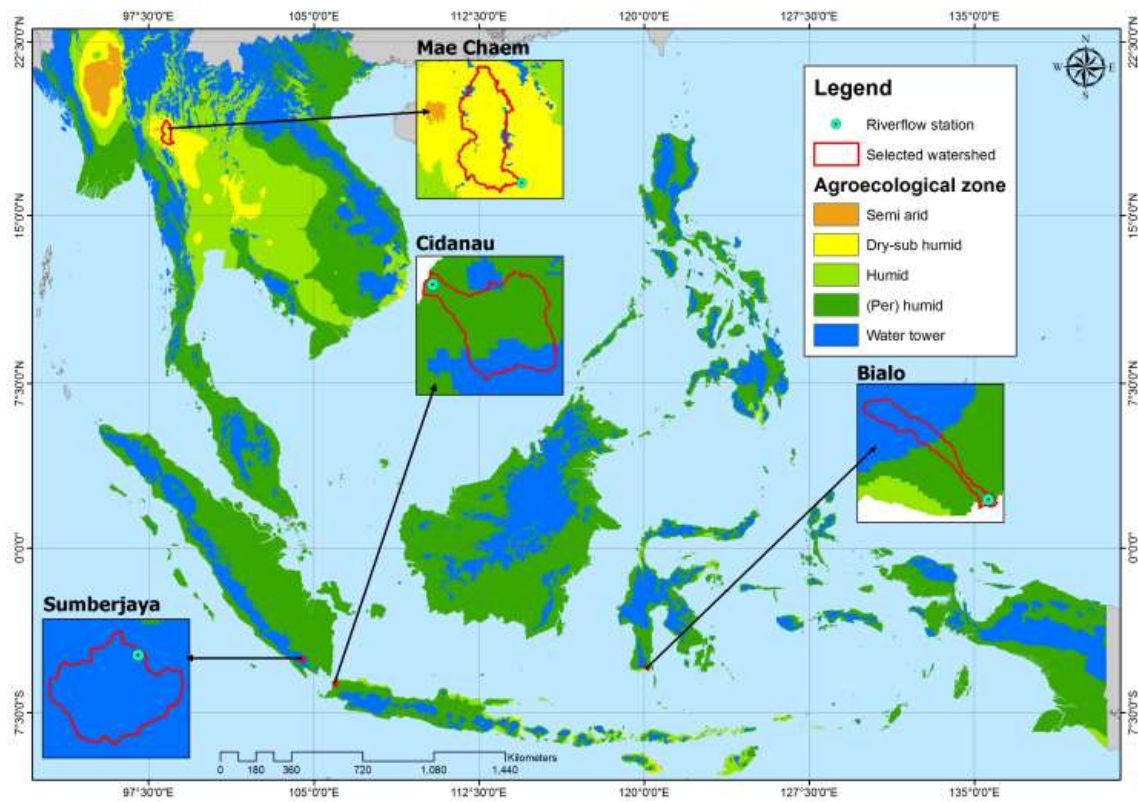
1152

1153   Figure 1. Location of the four watersheds in the agroecological zones of Southeast Asia
1154   (water towers are defined on the basis of ability to generate riverflow and being in the
1155   upper part of a watershed)

1156
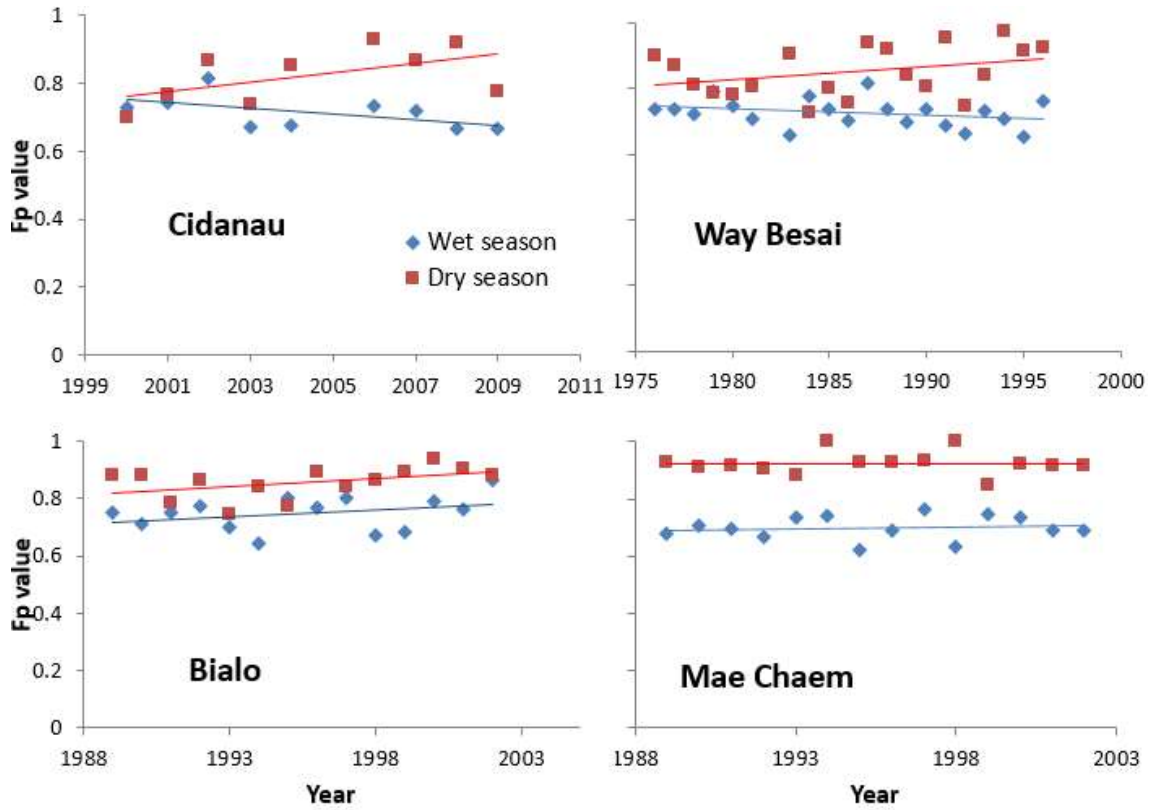
1159   Figure 2. Flow persistence (F_p) estimates derived from measurements in four watersheds,
1160   separately for the wettest and driest 3-month periods of the year

1161

1162
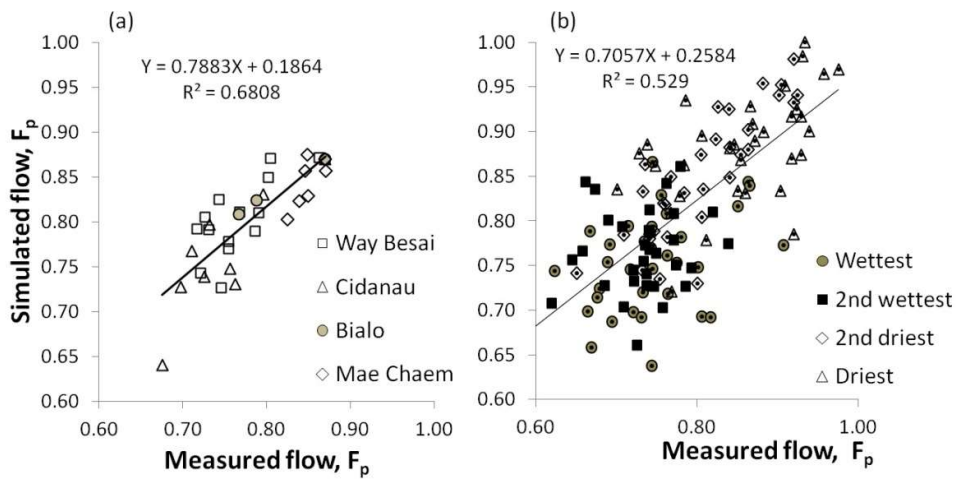
1163

1164   Figure 3. Inter- (A) and intra- (B) annual variation in the F_p parameter derived from empirical

1165   versus modeled flow: for the four test sites on annual basis (A) or three-monthly basis (B)

1166
1167
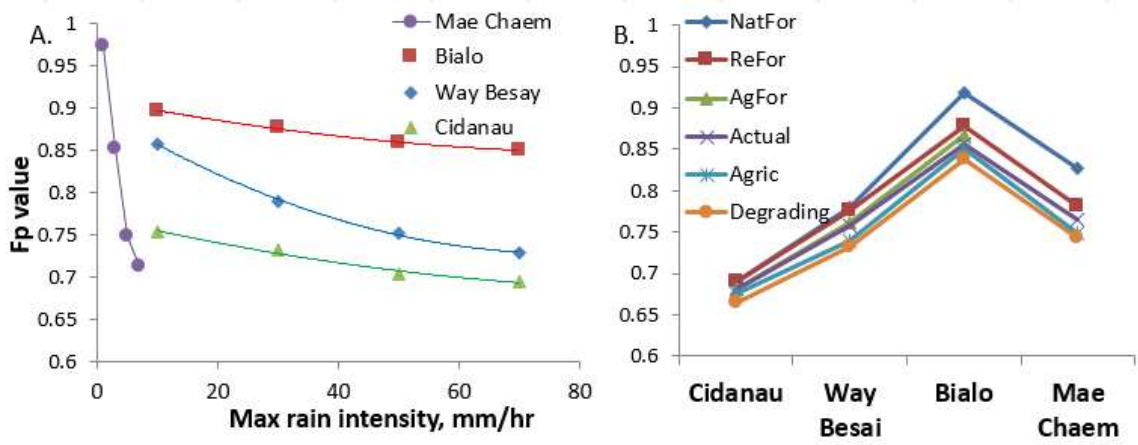
1168

1169 Figure 4 Effects on flow persistence of changes in A) the mean rainfall intensity and B) the

1170   land use change scenarios of Table 4 across the four watersheds

1171
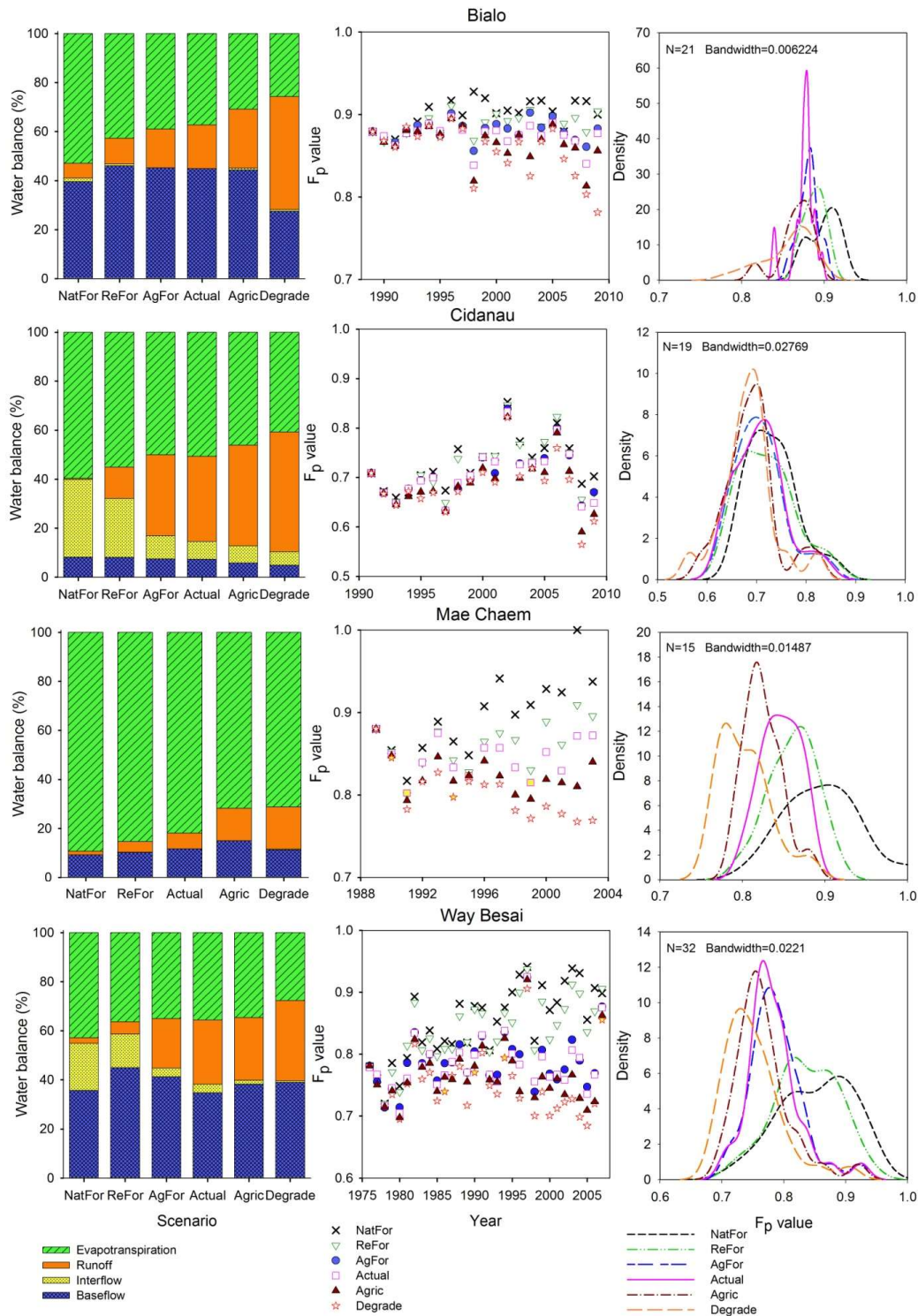
1172

1173   Figure 5. Effects of land cover change scenarios (Table 4) on the flow persistence value in

1174   four watersheds, modelled in GenRiver over a 20-year time-period, based on actual rainfall

1175   records; the left side panels show average water balance for each land cover scenario, the

1176   middle panels the Fp values per year and land use, the right-side panels the derived

1177   frequency distributions (best fitting Weibull distribution)

1178
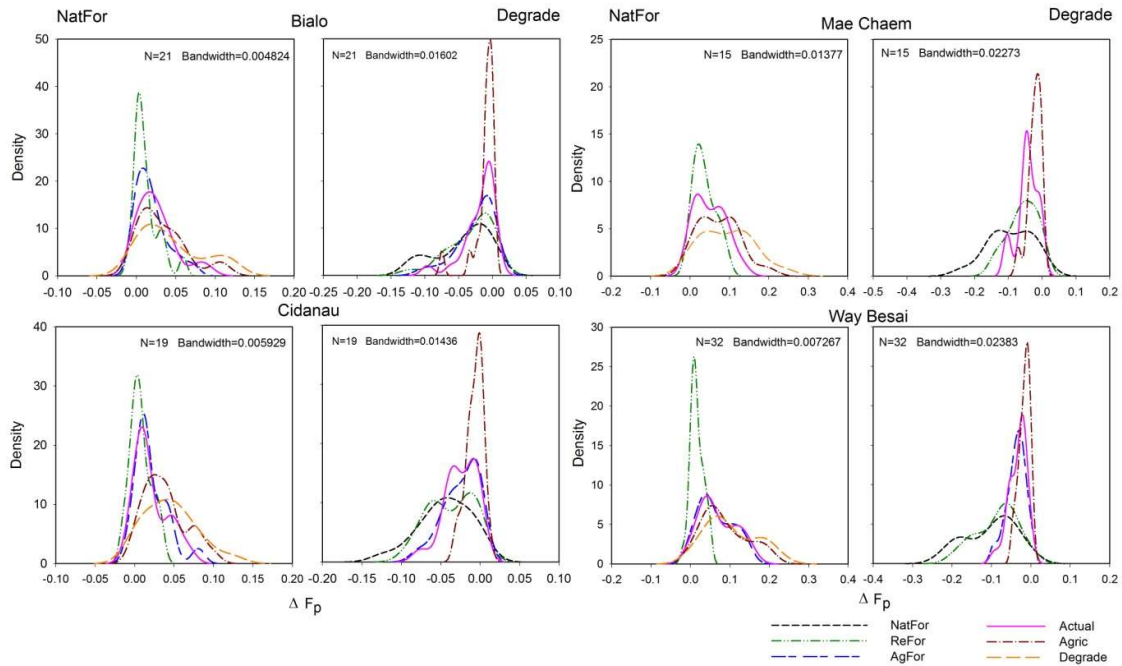
1179

1180   Figure 6. Frequency distribution of expected difference in F_p in 'paired plot' comparisons

1181   where land cover is the only variable; left panels: all scenarios compared to 'reforestation',

1182   righ panel: all scenarios compared to degradation; graphs are based on a kernel density

1183   estimation (smoothing) approach

1184
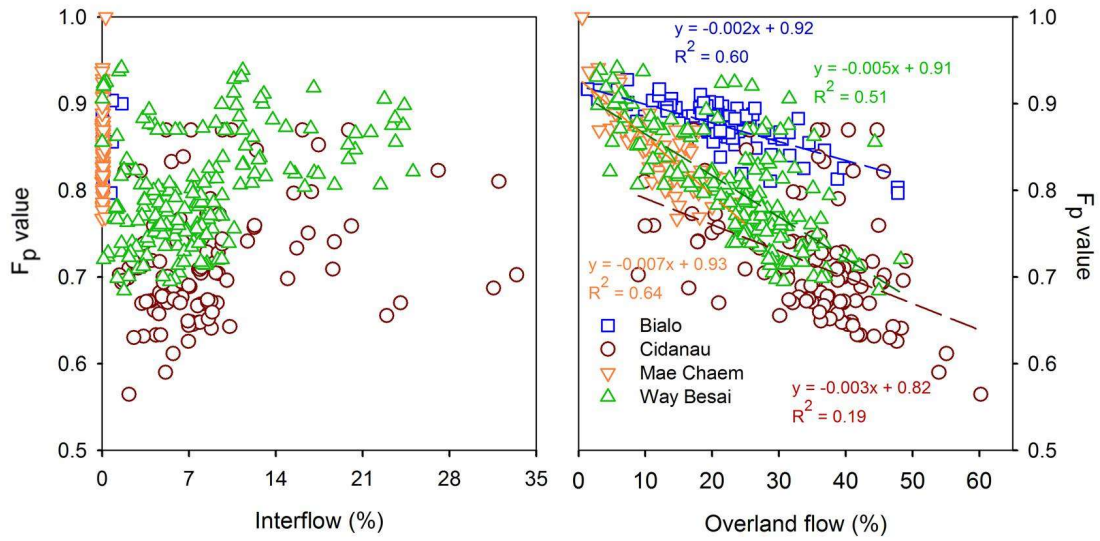
1185

1186   Figure 7. Correlations of F_p with fractions of rainfall that take overland flow and interflow

1187   pathways through the watershed, across all years and land use scenarios of Fig. App2

1188

1189

1190   Appendix 1. GenRiver model for effects of land cover on river flow

1191   The Generic Riverflow (GenRiver) model (van Noordwijk et al., 2011) is a simple

1192   hydrological model that simulates river flow based on water balance concept with a daily time

1193   step and a flexible spatial subdivision of a watershed that influences the routing of water. The

1194   core of the GenRiver model is a "patch" level representation of a daily water balance, driven

1195   by local rainfall and modified by the land cover and land-cover change and soil properties.

1196   The model starts accounting of rainfall or precipitation (P) and traces the subsequent flows

1197   and storage in the landscape that can lead to either evapotranspiration (E), river flow (Q) or

1198   change in storage (ΔS) (Figure App1):

1199 $P = Q + E + \Delta S$ [1]
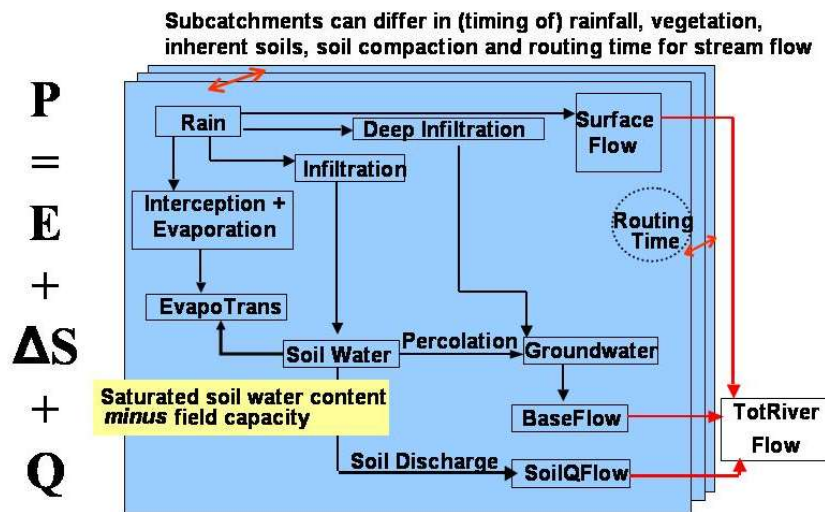
Figure App1.Overview of the GenRiver model

1200

1201   The model may use measured rainfall data, or use a rainfall generator that involves Markov

1202   chain temporal autocorrelation (rain persistence). The model can represent spatially explicit

1203   rainfall, with stochastic rainfall intensity (parameters RainIntensMean, RainIntensCoefVar in

1204   Table 2) and partial spatial correlation of daily rainfall between subcatchments. Canopy

1205   interception leads to direct evaporation of an amount of water controlled by the thickness of

1206   waterfilm on the leaf area that depends on the land cover, and a delay of water reaching the

1207   soil surface (parameter RainMaxIntDripDur in Table 2). The effect of evaporation of intercepted

1208   water on other components of evapotranspiration is controlled by the InterceptEffectontrans

1209   parameter, that in practice may depend on the time of day rainfall occurs and local climatic conditions

1210   such as windspeed)

1211   At patchlevel, vegetation influences interception, retention for subsequent evaporation and

1212   delayed transfer to the soil surface, as well as the seasonal demand for water. Vegetation (land

1213   cover) also influences soil porosity and infiltration, modifying the inherent soil properties.

1214   Groundwater pool dynamics are represented at subcatchment rather than patch level,

1215   integrating over the landcover fractions within a subcatchment. The output of the model is

1216   river flow which is contribution from three types of stream flow: surface flow on the day of

1217   the rainfall event; interflow on the next day; and base flow as the slow flow. the multiple

1218   subcatchments that make up the catchment as a whole can differ in basic soil properties, land-

1219   cover fractions that affect interception, soil structure (infiltration rate) and seasonal pattern of

1220   water use by the vegetation. The subcatchment will also typically differ in "routing time" or

1221   in the time it takes the streams and river to reach any specified observation point (with default

1222   focus on the outflow from the catchment). The model itself (currently implemented in Stella

1223   plus Excel), a manual and application case studies are freely available

1224   (http://www.worldagroforestry.org/output/genriver-genetic-river-model-river-flow   ;van

1225   Noordwijk et al., 2011).

1226

1227 Appendix 2. Watershed-specific consequences of the land use change scenarios

1228 The generically defined land use change scenarios (Table 4) led to different land cover

1229 proportions, depending on the default land cover data for each watershed, as shown in Fig.

1230 App2.
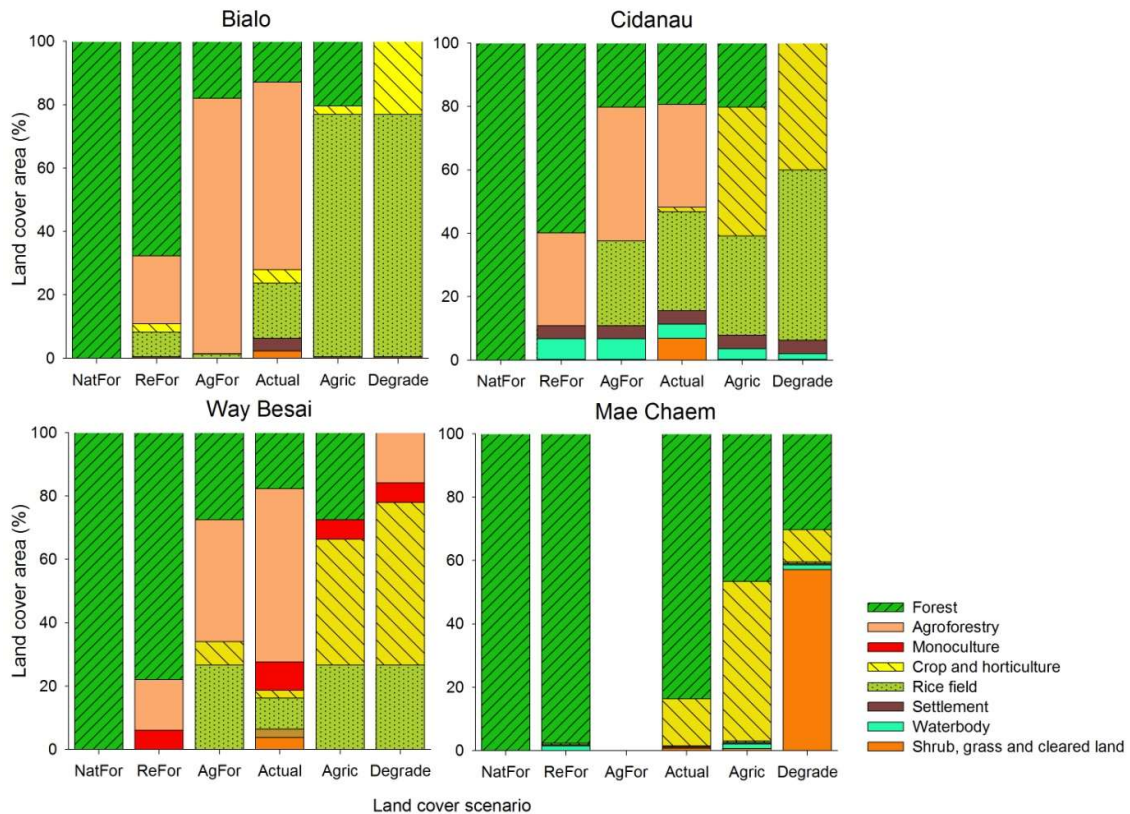
1231
1232 Figure App2. Land use distribution of the various land use scenarios explored for the four

1233 watersheds (see Table 4)

1234

1235   Appendix 3. Example of a macro in R to estimate number of observation required using

1236   bootstrap approach.

1237

```
1238    #The bootstrap procedure is to calculate the minimum sample size (number of observation) required
1239    #for a significant land use effect on Fp
1240    #bialo1 is a dataset contains delta Fp values for two different from Bialo watershed
1241
1242    #read data
1243    bialo1 <- read.table("bialo1.csv", header=TRUE, sep=",")
1244
1245    #name each parameter
1246    BL1 <- bialo1$ReFor
1247    BL5 <- bialo1$Degrade
1248
1249    N = 1000 #number replication
1250
1251    n <- c(5:50) #the various sample size
1252
1253    J <- 46 #the number of sample size being tested (~ number of actual year observed in the dataset)
1254
1255    P15= matrix(ncol=J, nrow=R) #variable for storing p-value
1256    P15Q3 <- numeric(J) #for storing p-Value at 97.5 quantile
1257
1258    for (j in 1:J) #estimating for different n
1259
1260    #bootstrap sampling
1261    {
1262    for (i in 1:N)
1263    {
1264    #sampling data
1265    S1=sample(BL1, n[j], replace = T)
1266    S5=sample(BL5, n[j], replace = T)
1267
1268    #Kolmogorov-Smirnov test for equal distribution and get the p-Value
1269    KS15 <- ks.test(S1, S5, alt = c("two.sided"), exact = F) P15[i,j] <- KS15$p.value
1270    }
1271
1272    #Confidence interval of CI
1273    P15Q3[j] <- quantile(P15[,j], 0.975)
1274
1275    }
1276
1277    #saving P value data and CI
1278
1279    write.table(P15, file = "pValue15.txt") write.table(P15Q3, file = "P15Q3.txt")v
```